Geological Evolution of the Red Sea: Historical Background, Review, and Synthesis

William Bosworth

Abstract

The Red Sea is part of an extensive rift system that includes from south to north the oceanic Sheba Ridge, the Gulf of Aden, the Afar region, the Red Sea, the Gulf of Aqaba, the Gulf of Suez, and the Cairo basalt province. Historical interest in this area has stemmed from many causes with diverse objectives, but it is best known as a potential model for how continental lithosphere first ruptures and then evolves to oceanic spreading, a key segment of the Wilson cycle and plate tectonics. Abundant and complementary datasets, from outcrop geology, geochronologic studies, refraction and reflection seismic surveys, gravity and magnetic surveys, to geodesy, have facilitated these studies. Magnetically striped oceanic crust is present in the Gulf of Aden and southern Red Sea, active magma systems are observed onshore in the Afar, highly extended continental or mixed crust submerged beneath several kilometers of seawater is present in the northern Red Sea, and a continental rift is undergoing uplift and exposure in the Gulf of Suez. The greater Red Sea rift system therefore provides insights into all phases of rift-to-drift histories. Many questions remain about the subsurface structure of the Red Sea and the forces that led to its creation. However, the timing of events—both in an absolute sense and relative to each other—is becoming increasingly well constrained. Six main steps may be recognized: (1) plume-related basaltic trap volcanism began in Ethiopia, NE Sudan (Derudeb), and SW Yemen at $\sim$31 Ma, followed by rhyolitic volcanism at $\sim$30 Ma. Volcanism thereafter spread northward to Harrats Sirat, Hadan, Ishara-Khirsat, and Ar Rahat in western Saudi Arabia. This early magmatism occurred without significant extension or at least none that has yet been demonstrated. It is often suggested that this "Afar" plume triggered the onset of Aden–Red Sea rifting, or in some models, it was the main driving force. (2) Starting between $\sim$29.9 and 28.7 Ma, marine syn-tectonic sediments were deposited on continental crust in the central Gulf of Aden. Therefore, Early Oligocene rifting is established to the east of Afar. Whether rifting propagated from the vicinity of the Sheba Ridge toward Afar, or the opposite, or essentially appeared synchronously throughout the Gulf of Aden is not yet known. (3) By $\sim$27.5–23.8 Ma, a small rift basin was forming in the Eritrean Red Sea. At approximately the same time ($\sim$25 Ma), extension and rifting commenced within Afar itself. The birth of the Red Sea as a rift basin is therefore a Late Oligocene event. (4) At $\sim$24–23 Ma, a new phase of volcanism, principally basaltic dikes but also layered gabbro and granophyre bodies, appeared nearly synchronously throughout the entire Red Sea, from Afar and Yemen to northern Egypt. The result was that the Red Sea rift briefly linked two very active volcanic centers covering 15,000–25,000 km^2 in the north and >600,000 km^2 in the south. The presence of the "mini-plume" in

W. Bosworth (✉)
Apache Egypt Companies, 11 Street 281, New Maadi
Cairo, Egypt
e-mail: bill.bosworth@apachecorp.com

N.M.A. Rasul and I.C.F. Stewart (eds.), *The Red Sea*,
Springer Earth System Sciences, DOI 10.1007/978-3-662-45201-1_3,

northern Egypt may have played a role somewhat analogous to Afar vis-à-vis the triggering of the dike event. The 24–23 Ma magmatism was accompanied by strong rift-normal extension and deposition of syn-tectonic sediments, mostly of marine and marginal marine affinity. The area of extension in the north was very broad, on the order of 1,000 km, and much narrower in the south, about 200 km or less. Throughout the Red Sea, the principal phase of rift shoulder uplift and rapid syn-rift subsidence followed shortly thereafter. Synchronous with the appearance of extension throughout the entire Red Sea, relative convergence between Africa and Eurasia slowed by about 50 %. (5) At ~14–12 Ma, a transform boundary cut through Sinai and the Levant continental margin, linking the northern Red Sea with the Bitlis–Zagros convergence zone. This corresponded with collision of Arabia and Eurasia, which resulted in a new plate geometry with different boundary forces. Red Sea extension changed from rift normal (N60°E) to highly oblique and parallel to the Aqaba–Levant transform (N15°E). Extension across the Gulf of Suez decreased by about a factor of 10, and convergence between Africa and Eurasia again dropped by about 50 %. In the Afar region, Red Sea extension shifted from offshore Eritrea to west of the Danakil horst, and activity began in the northern Ethiopian rift. (6) These early events or phases all took place within continental lithosphere and formed a continental rift system 4,000 km in length. When the lithosphere was sufficiently thinned, an organized oceanic spreading center was established and the rift-to-drift transition started. Oceanic spreading initiated first on the Sheba Ridge east of the Alula-Fartaq fracture zone at ~19–18 Ma. After stalling at this fracture zone, the ridge probably propagated west into the central Gulf of Aden by ~16 Ma. This matches the observed termination of syn-tectonic deposition along the onshore Aden margins at approximately the same time. At ~10 Ma, the Sheba Ridge rapidly propagated west over 400 km from the central Gulf of Aden to the Shukra al Sheik discontinuity. Oceanic spreading followed in the south-central Red Sea at ~5 Ma. This spreading center was initially not connected to the spreading center of the Gulf of Aden. By ~3 to 2 Ma, oceanic spreading moved west of the Shukra al Sheik discontinuity, and the entire Gulf of Aden was an oceanic rift. During the last ~1 My, the southern Red Sea plate boundary linked to the Aden spreading center through the Gulf of Zula, Danakil Depression, and Gulf of Tadjoura. Presently, the Red Sea spreading center may be propagating toward the northern Red Sea to link with the Aqaba–Levant transform. However, important differences appear to exist between the southern and northern Red Sea basins, both in terms of the nature of the pre- to syn-rift lithospheric properties and the response to plate separation. If as favored here no oceanic spreading is present in the northern Red Sea, then it is a magma-poor hyperextended basin with β factor >4 that is evolving in many ways like the west Iberia margin. It is probable that the ultimate geometries of the northern and southern Red Sea passive margins will be very different. The Red Sea provides an outstanding area in which to study the rift-to-drift transition of continental disruption, but it is unlikely to be a precise analogue for all passive continental margin histories.

Introduction

The Red Sea has long been recognized as one component of a continent scale rift system that reaches from the Dead Sea to Mozambique. This lead to the popularization of the term "Afro-Arabian rift system" by geologists mapping its different segments (Baker 1970; Khan 1975; Kazmin 1977). It was suggested that the Red Sea, and similarly the Gulf of Aden, were oceanic rifts at divergent plate boundaries, with a triple junction located at Afar (Fig. 1; Gass 1970; McKenzie et al. 1970; Girdler and Darracott 1972; Burke and Dewey 1973; Le Pichon and Francheteau 1978). Application of plate tectonics has been a central theme in studies of the Red Sea since then.

In 1972, the R/V *Glomar Challenger* conducted Leg 23B in the Red Sea and drilled six wells (sites 225–230) in and nearby the axial trough (Whitmarsh et al. 1974). These wells confirmed that basalts and fluids with mantle-derived lead isotopes have been emplaced into the sediment column along the Red Sea axis and supported the hypothesis that the Red Sea was an evolving oceanic rift. As part of this project, Coleman (1974) compiled a geologic map of the entire Red Sea basin, volcanism of the rift margins, and axial hydrothermal deeps. Based on geological observations, Coleman

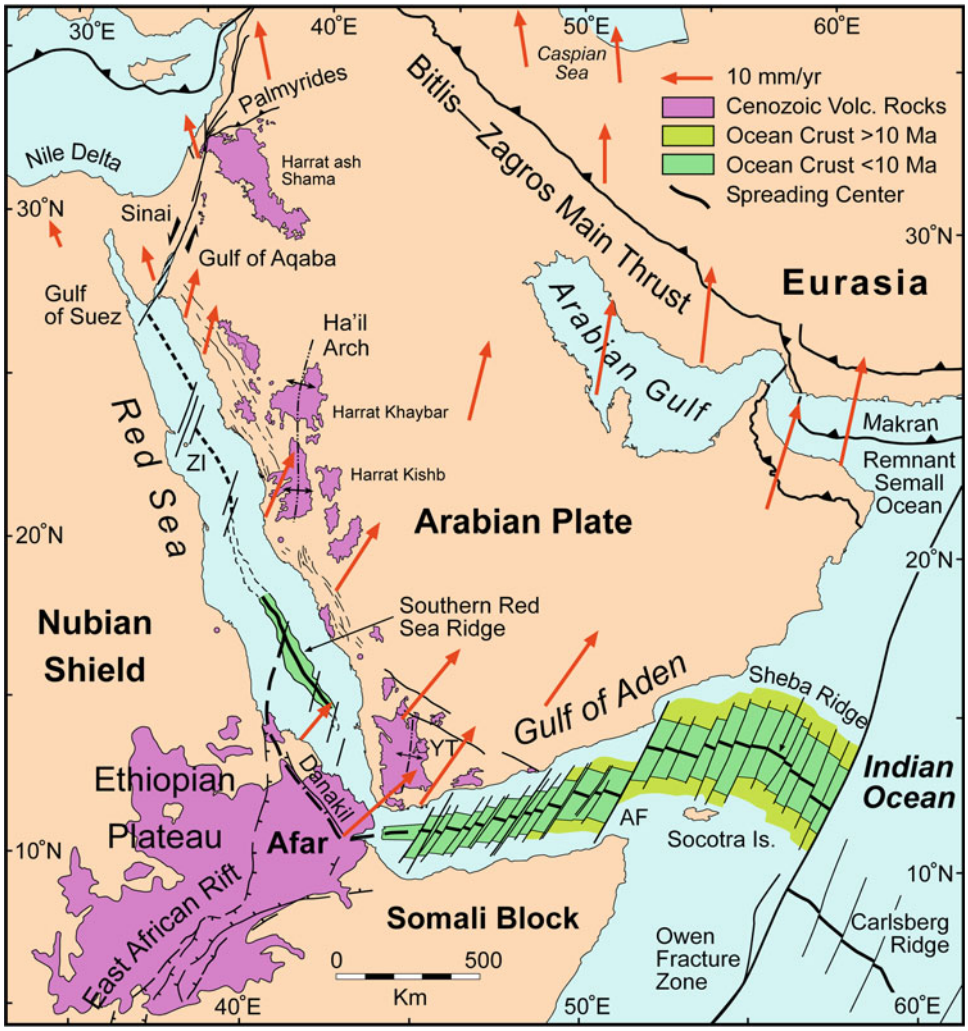

Fig. 1 Tectonic features of the greater Red Sea rift system, including the northern Ethiopian (East African) rift, Afar, and the Gulfs of Aden, Aqaba and Suez. After Bosworth et al. (2005). *AF* Alula-Fartak fracture zone, *YT* Yemen traps, *ZI* Zabargad Island. *Red arrows* are GPS velocities in a Eurasia-fixed reference frame from ArRajehi et al. (2010). Albers conical equal area projection

argued that oceanic crust was restricted to the axial trough in the southern Red Sea and that the rest of the margin was continental crust intruded by tholeiitic gabbros and basalt dike swarms. Similar interpretations had been developed from geophysical datasets (Girdler 1958; Drake and Girdler 1964; Lowell and Genik 1972). This contrasts with the McKenzie et al. (1970) model that envisioned a pre-rift coast-to-coast restoration with the entire Red Sea underlain by oceanic crust. Numerous intermediate models had also been proposed (Girdler 1966, 1970; Girdler and Darracott 1972).

The most convincing evidence of oceanic rifting was the recognition of striped magnetic anomalies along the southern Red Sea axis (Phillips 1970; Girdler and Styles 1974; Röser 1975; Searle and Ross 1975; Hall et al. 1977; Cochran 1983). These authors did not agree on the age of the anomalies when compared to world-wide magnetostratigraphy, but they did concur that the striping represents the signature of true oceanic spreading. Many other types of geophysical and geochemical data supported the oceanic rift scenario, and more details of these will be presented later in this chapter.

Just as it is firmly thought that the southern Red Sea is presently an oceanic rift, there is clear consensus that the northern end of the rift—the Gulf of Suez—is purely continental in character (Steckler 1985; Jarrige et al. 1986; Courtillot et al. 1987; Girdler and Southren 1987; Joffe and Garfunkel 1987; Moretti and Chénet 1987). The intervening areas—the central and northern Red Sea—have not met with similar agreement. In outcrop and in offshore exploratory wells, there are clear similarities with the Gulf of Suez, both in terms of stratigraphy and underlying basement lithologies (Colemen 1974; Tewfik and Ayyad 1984; Barakat and Miller 1984; Beydoun 1989; Beydoun and Sikander 1992; Bosworth 1993). Along the axial trough, however, there are some similarities with the southern Red Sea axis and some important differences (discussed below). Suffice it to say that the northern and central Red Sea are transitional between aborted continental rifting in the north and well-defined oceanic rifting in the south, though these areas may not represent a simple chronological progression now captured at different points in its evolution. Hence, the broad interest

in the Red Sea despite-or perhaps because of-its inherent geological and geophysical complexities.

Recent advances in radiometric dating of Red Sea volcanic samples, new thermochronologic studies, growing global positioning system (GPS) datasets, seismic tomography, and improved theoretical models have set the stage for significant revisions in the interpreted tectonic evolution of this rift system. Though understanding of the mechanisms responsible for the formation of the Red Sea will continue to improve, a much more refined chronology of events is now possible and synthesis of this information is the key theme of the present contribution. This chapter will start with a brief review of the geology of the Red Sea and will attempt to provide a concise but broad range of background material and appropriate references for more detailed information. Much of the material covered in recent reviews will not be included (Bosworth et al. 2005; Cochran 2005; Garfunkel and Beyth 2006; Lazar et al. 2012). Another invaluable source of data and syntheses about many aspects of the Red Sea is the book "*Geologic Evolution of the Red Sea*" by Coleman (1993). The chapter will then move to discussions of when did the Red Sea initiate and how did it evolve as a continental rift, what were the Red Sea's relationships to the Gulf of Aden, Gulf of Aqaba, and Ethiopian rifts, when did the transition to oceanic spreading occur, what caused the termination of the Red Sea in the north and the subsequent formation of the Levant transform boundary, and what were the forces responsible for the formation of the Red Sea.

The timescale of Gradstein et al. (2004) is used throughout this paper. Micropaleontologic interpretations based on the planktonic foraminiferal zones of Blow (1969) and the calcareous nannofossil zones of Martini (1971) have been adjusted to this timescale.

Geologic and Tectonic Setting

Background

Modern broad-scale geologic mapping of the margins of the Red Sea began in earnest as a cooperative program between the US Geological Survey and the Kingdom of Saudi Arabia that resulted in coverage and integration of data from all of the Arabian Peninsula (USGS-Arabian American Oil Company 1963; Geukens 1966; Greenwood and Bleackley 1967; Bender 1975; Brown et al. 1989). Brown (1972) produced a tectonic interpretation of these data that included the Red Sea coastal plain and bathymetry of the axial trough. Ethiopia and Djibouti also received extensive attention due to interest in the Afar flood basalts/plume, the Danakil Horst, and the Strait of Bab-al-Mandab (Brinckmann and Kursten 1969; Clin and Pouchan 1970; Barberi et al. 1971; Kazmin 1973). Further mapping was completed in Yemen (Grolier and Overstreet 1978), and similar compilations were published for the Sinai Peninsula (Eyal et al. 1980) and later the western Gulf of Suez and Red Sea margin of Egypt (Klitzsch et al. 1986, 1987). The Sudan was not mapped as extensively as other countries bordering the Red Sea, though country-scale maps were produced (Vail 1975, 1978).

While the Red Sea margins were being systematically mapped onshore, exploratory drilling for hydrocarbons had commenced in both the onshore and offshore. Oil seeps had earlier been reported along the coastline at Gebel el Zeit, Gebel Tanka, and Abu Durba in the Gulf of Suez, north of Massawa and at the Dahlak Islands in the Sudan, near Zeidiye in Yemen, and in Saudi Arabia at the Farasan Islands, north of Yanbu and at Midyan (Hume et al. 1920; Beydoun 1989; Bunter and Abdel Magid 1989; Egyptian General Petroleum Corporation 1996). By 1987, 10 wells had been drilled offshore Egypt, 11 offshore Sudan, 18 offshore Ethiopia (includes some very shallow on the Dahlak Islands), 5 offshore Yemen, and 13 offshore Saudi Arabia (includes some very shallow on the Farasan Islands) (Beydoun 1989; Beydoun and Sikander 1992). Since then, 4 deepwater wells have been drilled along the Egyptian margin and an undisclosed number of wells offshore Saudi Arabia. These drilling campaigns have established the general stratigraphy of the Red Sea basin and verified correlations with the Gulf of Suez and Gulf of Aden syn-rift sections (reviewed in Bosworth et al. 2005). Unfortunately, productive hydrocarbon systems have only been discovered in the Midyan (both onshore and offshore) and Al Wajh/Umm Luj basins of Saudi Arabia and the Tokar–Suakin delta of the Sudan.

Africa's Other Rifts and the Red Sea

The evolution of the Red Sea should be considered in the context of the entire African plate. This can be discussed from several perspectives. Africa is a remnant of Gondwana, which began to break up during the Late Carboniferous starting with "Karoo" rifts in southern and east Africa (Groenewald et al. 1991; Bumby and Guiraud 2005). Diachronous Early Permian rifting occurred along the northern African margin from Morocco to Egypt, resulting in the initiation of the Neotethyan seaway (Stampfli and Borel 2002). By the Middle Triassic, seafloor spreading was probably occurring in the eastern Mediterranean basin (Robertson et al. 1996; Stampfli et al. 2001). Rifting began along the Central Atlantic margins in the Late Triassic (Davison 2005). During the Jurassic, extension spreads to the inboard basins of the Neotethyan margin (Guiraud and Bosworth 1999), the Blue Nile rift in Sudan (Wycisk et al. 1990; Bosworth 1992), the Marib-Shabwa basin in Yemen (Bott et al. 1992), the Nogal rift of Somalia (Granath 2001), the Lamu embayment of Kenya (Reeves et al. 1987) and continued in the Karoo Lugh-Mandera basin of

Kenya–Somalia–Ethiopia (Ali Kassim et al. 2002). Seafloor spreading initiated along the Central Atlantic margins in the Early Jurassic (~180 Ma; Klitgord and Schouten 1986; Davison 2005) and in the Somali basin in the Middle to Late Jurassic (pre-157 Ma; Rabinowitz et al. 1983). By the Late Jurassic, faulting was active in the Benue trough in Nigeria (Guiraud 1993) and was present throughout the South Atlantic basin by the Early Cretaceous (Rabinowitz and LaBreque 1979). Seafloor spreading initiated in the South Atlantic in the Neocomian to Aptian, progressing from south to north (Uchupi 1989) and in the equatorial Atlantic in the Late Aptian (~115 Ma; Basile et al. 2005). By this time, the present geometry of the African plate was essentially established. Through the Cretaceous and locally into the Cenozoic, however, continental extension continued in many African basins, particularly within the Benue trough, the Termit basin of Niger, the Dobaa basin of Chad, the south Sudan rifts, the Anza trough, the Sirte basin of Libya, the Western Desert of Egypt, and the basins of Yemen and Somalia (Fairhead 1988; Genik 1992; Guiraud and Maurin 1992; Bosworth 1992, 1994; Janssen et al. 1995; Bumby and Guiraud 2005; Guiraud et al. 2005). In summary, the breakup/dispersal of the Gondwana segment of Pangaea lasted several hundred million years. The Red Sea–Gulf of Aden rift system, with the East African rifts, is part of this ongoing process (Bumby and Guiraud 2005; Bosworth et al. 2005).

The driving mechanism for the breakup of a supercontinent such as Pangaea has been attributed to thermal blanketing of the underlying mantle and related plume or hotspot activity impinging on the base of the lithosphere (Anderson 1982). Slab retreat and slab pull on surrounding plate boundaries have also been suggested as associated principal driving forces (Davies and Richards 1992; Lithgow-Bertelloni and Richards 1998; Collins 2003; Reilinger and McClusky 2011). Both plumes and nearby subduction zone processes probably played key roles in the evolution of the Red Sea (reviewed in Bosworth et al. 2005). Plumes weaken continental lithosphere and therefore may strongly influence the location of lithospheric failure, while plate boundary forces can drive extension.

This brief overview illustrates the dominant tectonic activity in Africa over the past 300 My—rifting and formation of passive continental margins. However, it has been suggested that this general theme has been modified during the most recent 30 My of its progression (Burke 1996). Early in the past century, geologists recognized that Africa possesses a distinctive basin and swell geomorphology (Krenkel 1922, 1957; Argand 1924; Holmes 1965). Following Krenkel, Burke and Wilson (1972) suggested that this topography was generated by mantle processes, while the African plate was essentially at rest with respect to the underlying pattern of mantle circulation. "Stationary Africa" arose ~30 Ma (Burke 1996) and has been attributed to intensified collision between Africa and Eurasia (Bailey 1992, 1993) and/or the impingement and eruption of the Afar plume, which possibly in conjunction with the Principe and other plumes acted to pin the base of the lithosphere to the upper mantle (Burke 1996). Burke suggested that the arresting of Africa plate motion led to a surge in intraplate volcanism and to renewed rifting, that is, formation of the Red Sea–Gulf of Aden–East Africa rift system (Afro-Arabia rift system). From about the end of the Cretaceous up until the development of stationary Africa, intraplate extension was absent or very localized across Africa, a gap in the rifting history of ~35 Ma. This gap was a period of major peneplanation (Burke 1996; Burke and Gunnell 2008) including the development of extensive laterites and paleosols across the Arabian–Nubian shield (Coleman 1993). This African surface was the backdrop on which the Red Sea was formed.

Geomorphology, Axial Deeps, and Rift Shoulder Uplift

The most prominent geomorphologic features of the Red Sea are the extreme deeps along the basin axis and the high elevations along most of its rifted shoulder (Fig. 2). Mapping compiled by Laughton (1970) revealed a continuous main axial trough that extends from just south of Ras Mohammed in southernmost Sinai to the vicinity of the Zubayr Islands offshore Yemen. The main trough is generally 1000 m or greater in depth and is accentuated by isolated deeps that exceed 2000 m (Degens and Ross 1969; Monin et al. 1981, 1982). The axial deeps contain hot brine pools and basaltic cones, some of which have been studied by detailed side beam sonar and direct sampling (Pautot 1983; Pautot et al. 1984; Bicknell et al. 1986) and are the subject of other chapters in this book. The deeps are intimately related to the evolution of oceanic spreading centers in the Red Sea (Cochran 1983; Bonatti 1985; Martinez and Cochran 1988; Cochran and Martinez 1988, reviewed in Cochran 2005; Cochran and Karner 2007).

Cochran (2005) compiled all the available bathymetric data for the Northern Red Sea (Fig. 2b) and integrated this with gravity and magnetic data to produce a new model for the nucleation of an oceanic spreading center at the axial depression. An interesting detail of his bathymetric map (present in older maps but not as refined) is the fact that the axial trough strikes 5°–10° more to the northwest than the overall trend of the marine basin. This may reflect an adjustment to extension parallel to the Gulf of Aqaba transform boundary (Bosworth et al. 2005; Lazar et al. 2012, discussed below) and is an expected consequence of the two Eulerian pole Red Sea opening models proposed by many authors (e.g., Joffe and Garfunkel 1987 and references therein).

The marine shelf and coastal plains of the Red Sea are variable in width and were formed by a complex interplay of tectonic, sedimentary, and biotic activity. The present climate

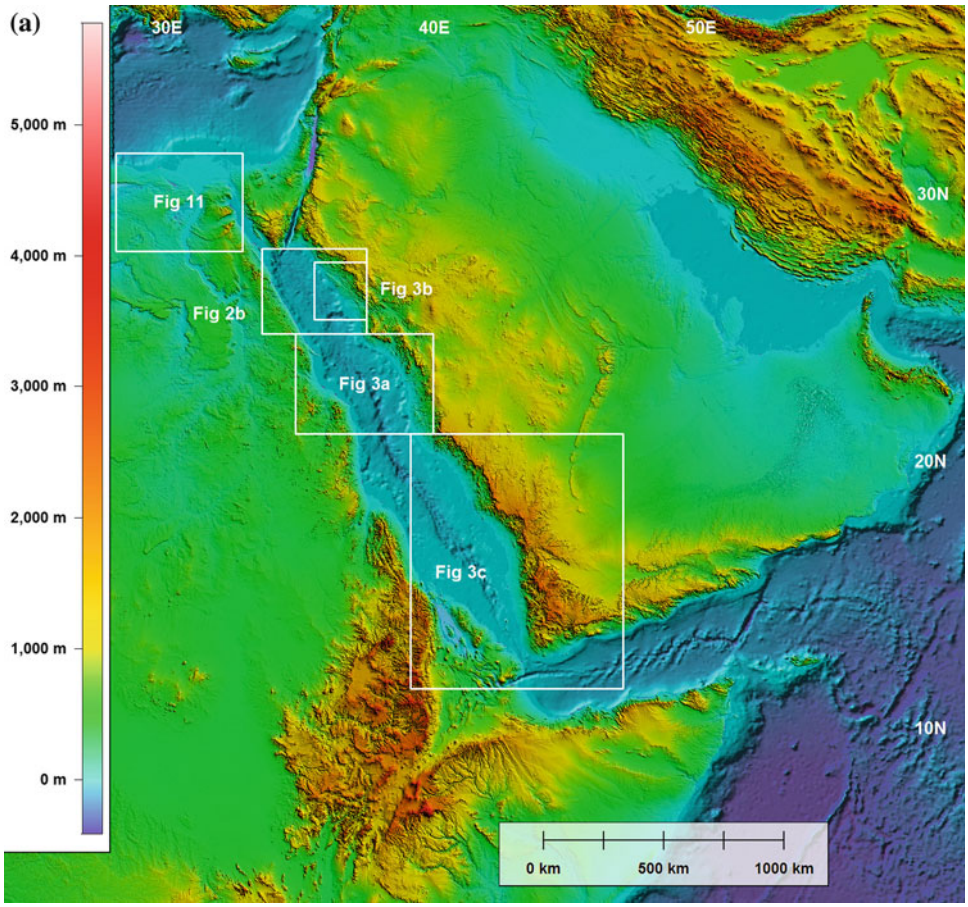

Fig. 2 Topography and bathymetry of the Red Sea area (geographic projection). **a** From GLOBE Task Team et al. (1999) (onshore) and Smith and Sandwell (1997) (offshore; Seasat radar altimetry derived bathymetry). Compared with Fig. 1 for positions of plate boundaries, Red Sea volcanic terranes and place names. Locations of other figures are given. **b** Detailed bathymetry of northern Red Sea from Cochran (2005). Onshore is same dataset as in (**a**). Topographic–bathymetric profile runs from 26°15′N, 33°30′E to 28°N, 37°E through the Conrad deep

of the entire Red Sea region is arid, with the exception of localized mountainous areas where increased rainfall due to orographic forcing results in increased vegetation (Zahran and Willis 2009). These areas are sometimes referred to as "mist oases" such as at Mt. Elba, Egypt (1,435 m; Kassas and Zahran 1971). No permanent rivers enter into the basin, though intermittent rivers such as the Barka (or Baraka) in the Red Sea Hills of Sudan (Fig. 3a) exist (Beydoun 1989). The Barka forms the Tokar delta at the coastline, and during the wetter pluvial stages of the Pleistocene, this probably was a constantly flowing river. Similarly, many dry wadis that now reach the Red Sea and deliver little sedimentation would have been more significant input points in the past. This is an important concept in the hydrocarbon exploration strategies employed in both the Gulf of Suez and the Red Sea (Richardson and Arthur 1988; Lambiase and Bosworth 1995). Offshore from Tokar several exploration wells have been drilled, and significant (though presently noncommercial) quantities of gas were discovered in a very thick sedimentary package that has been referred to as the Suakin delta.

The southern coastlines of both the Arabian and African Red Sea margins are curvilinear and paired and reflect the initial rift geometry of the basin. North of about 24° latitude however on both sides of the basin, the shorelines are linear (Figs. 2b, 3b), and as discussed below, this does not reflect the original shape of the rift. It has been suggested that the straight coasts may be the result of young basement-involved faulting (Bosworth 1994; Bosworth and Burke 2005). The youngest faults actually observed in reflection seismic data offshore from these areas generally detach within the Middle and Late Miocene halite units (Mougenot and Al-Shakhis 1999; Bosworth and Burke 2005). Gravity-driven detached faults would probably produce a scalloped coastline, and there is not any active seismicity near the coast to support the basement-fault model. The straight northern coasts remain somewhat enigmatic.

Inland from coastal plains, or in many areas immediately adjacent to the coastline, high elevations are encountered along most of the Red Sea. From Taif (Saudi Arabia) to Taizz (Yemen) along the Arabian margin, the high terrain is bounded by an unbroken erosional escarpment with the highest peaks exceeding 3,000 m (Fig. 3a, c; Spohner and Oleman 1986; Bohannon 1986; Coleman 1993). In Ethiopia, the escarpment marks the eastern edge of the Ethiopian plateau, with elevations in excess of 2,000 m (Fig. 2a). The geomorphology in Afar is made more complex by the presence of the Danakil horst near the coast and the Afar depression itself (Figs. 1, 2a, 3c; Barberi et al. 1972). Along

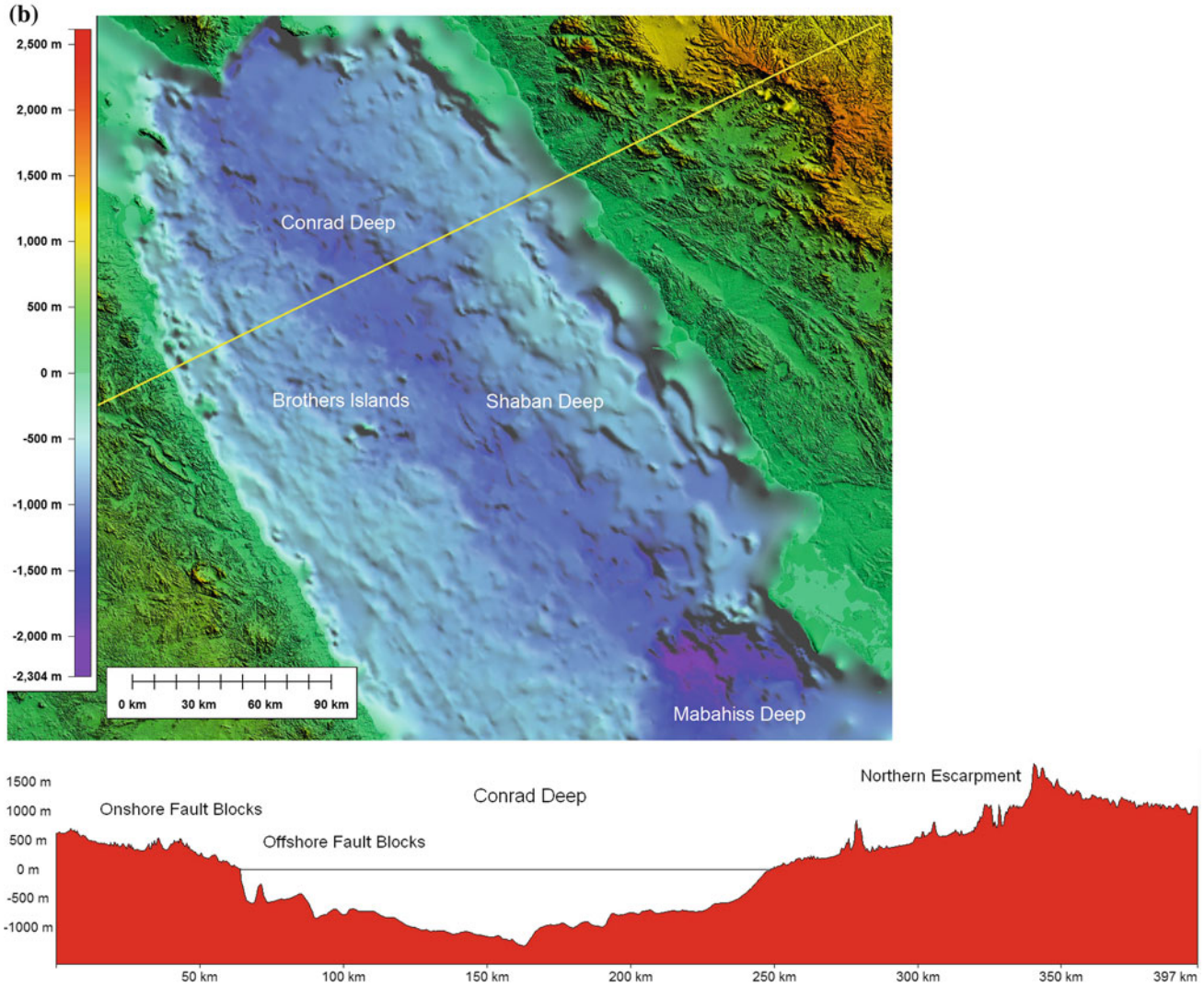

Fig. 2 (continued)

the Sudan margin, the elevation in the Red Sea Hills is more subdued but still typically greater than 1,000 m. This magnitude of relief continues north to Egypt and along the western margin of the Gulf of Suez, with isolated basement peaks reaching 1,400 to more than 2,000 m (Gebel Gharib 1,757 m; Gebel Shaayib Al-Banat 2,187 m). The elevation on Sinai is greater, with Mt. Sinai itself 2,285 m and nearby Mt. St. Catherine 2,629 m (Figs. 2a, 4).

The timing and causes of the uplift of the margins of the Red Sea and Gulf of Suez have long been debated. Gass (1970) and later other workers suggested that the region of Afar was uplifted prior to rifting during the Oligocene or even earlier. Apatite fission track cooling dates were first obtained for the basement complex of Sinai (Kohn and Eyal 1981) and indicated that an important period of denudation occurred between ~27 and 20 Ma. However, most of the dates clustered at 22–20 Ma. Data from the western margin of the Gulf were similarly centered at 22 ± 1 Ma (Omar et al. 1989). Along the Saudi Arabian southern Red Sea margin, Bohannon (1986) suggested that uplift was coeval with faulting at about 25–23 Ma, with a total of ~3.5 km of unroofing. Later interpretations by Bohannon et al. (1989) envisioned initial erosion and uplift at 20 Ma, but with at least 2.5 km of the total occurring after 13.8 Ma. Apatite (U-Th)/He thermochronometry from exposed footwall blocks in the central Saudi Arabian margin indicated rapid exhumation at ~22 Ma and a second distinct pulse about 8 Ma later (Szymanski 2013).

For the Yemeni margin, exhumation was identified at 17–16 Ma (Menzies et al. 1992, 1997), but on the conjugate margin in Eritrea, Abbate et al. (2002) found a broad range of fission track ages (400–10 Ma). Modeling did suggest, however, a major crustal cooling event driven by denudation at 20 Ma. Ghebreab et al. (2002) also found cooling ages along the Eritrean margin north of Danakil clustering between 23 and 17 Ma.

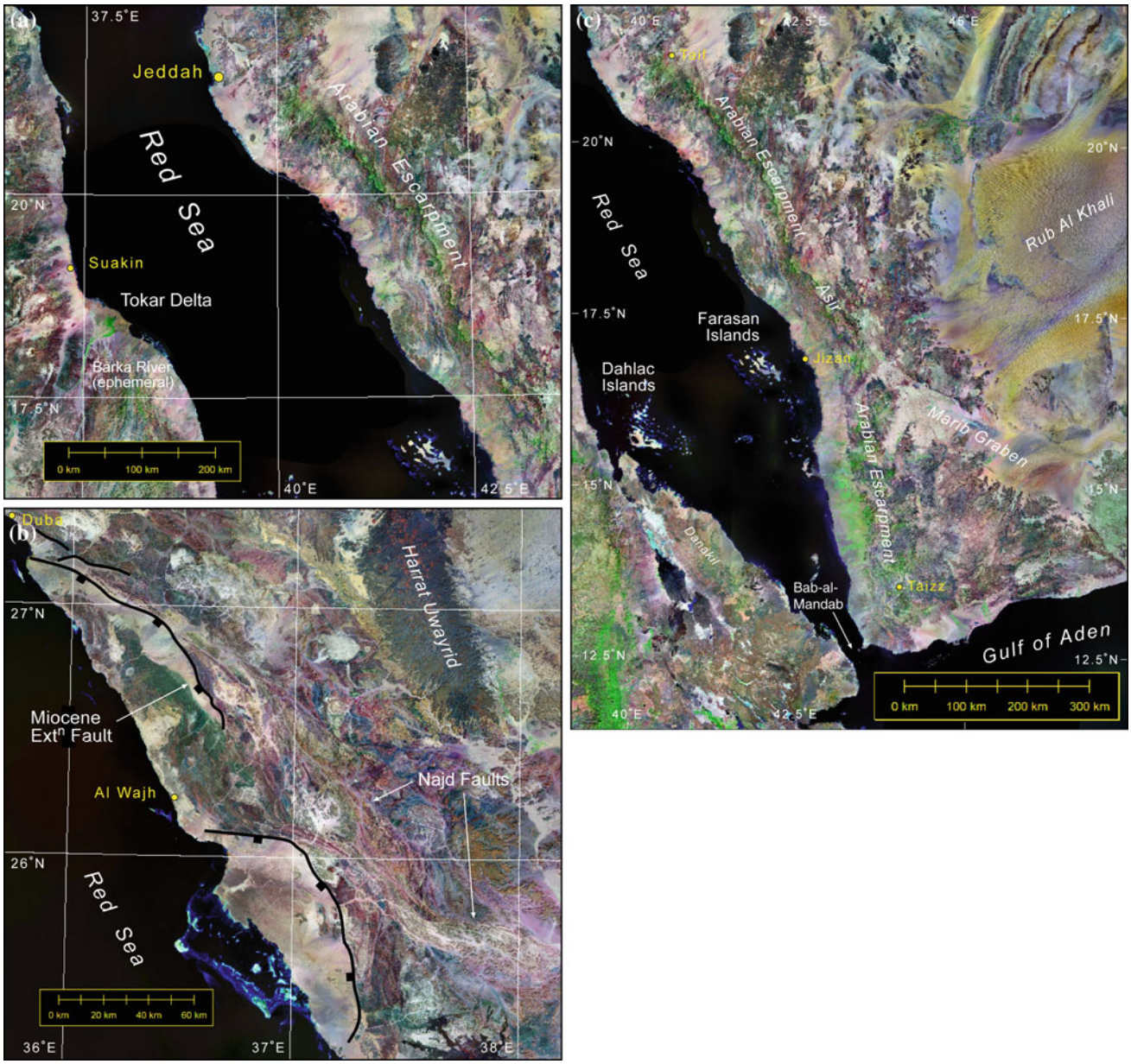

Fig. 3 Landsat 7 mosaics of the Red Sea margins (transverse Mercator projections): **a** The Arabian escarpment south of Jeddah, Saudi Arabia, and the Tokar delta at the mouth of the ephemeral Barka River south of Suakin, Sudan. **b** Miocene extensional faults near Duba and Al Wajh, Saudi Arabia that reactivated parts of the Neoproterozoic Najd fault system. **c** The Arabian escarpment from Taif, Saudi Arabia to Taizz, Yemen. Imagery is from the NASA Stennis Space Center GeoCover project (MDA Federal 2004)

Taken in their entirety, the fission track and (U-Th)/He data suggest that the rift flanks of the Red Sea began denudation at about 24–23 Ma, at least locally, and by about 22–20 Ma, fairly continuous rift shoulders were present. Some fission track data have been produced that suggest an even earlier unroofing event, at ~34 Ma—in the Late Eocene (Steckler and Omar 1994; Omar and Steckler 1995). These data come from the western Gulf of Suez and Egyptian Red Sea margins. Bosworth and McClay (2001) suggested that this phase of uplift, if significant, was more likely related to the Late Eocene Syrian arc compressional phase that is well documented in these same areas (Guiraud and Bosworth 1999).

Large-Scale Basin Geometry

Utilizing wells drilled in the offshore Egyptian Red Sea margin, Tewfik and Ayyad (1984) and Barakat and Miller (1984) established that the Miocene stratigraphy of the

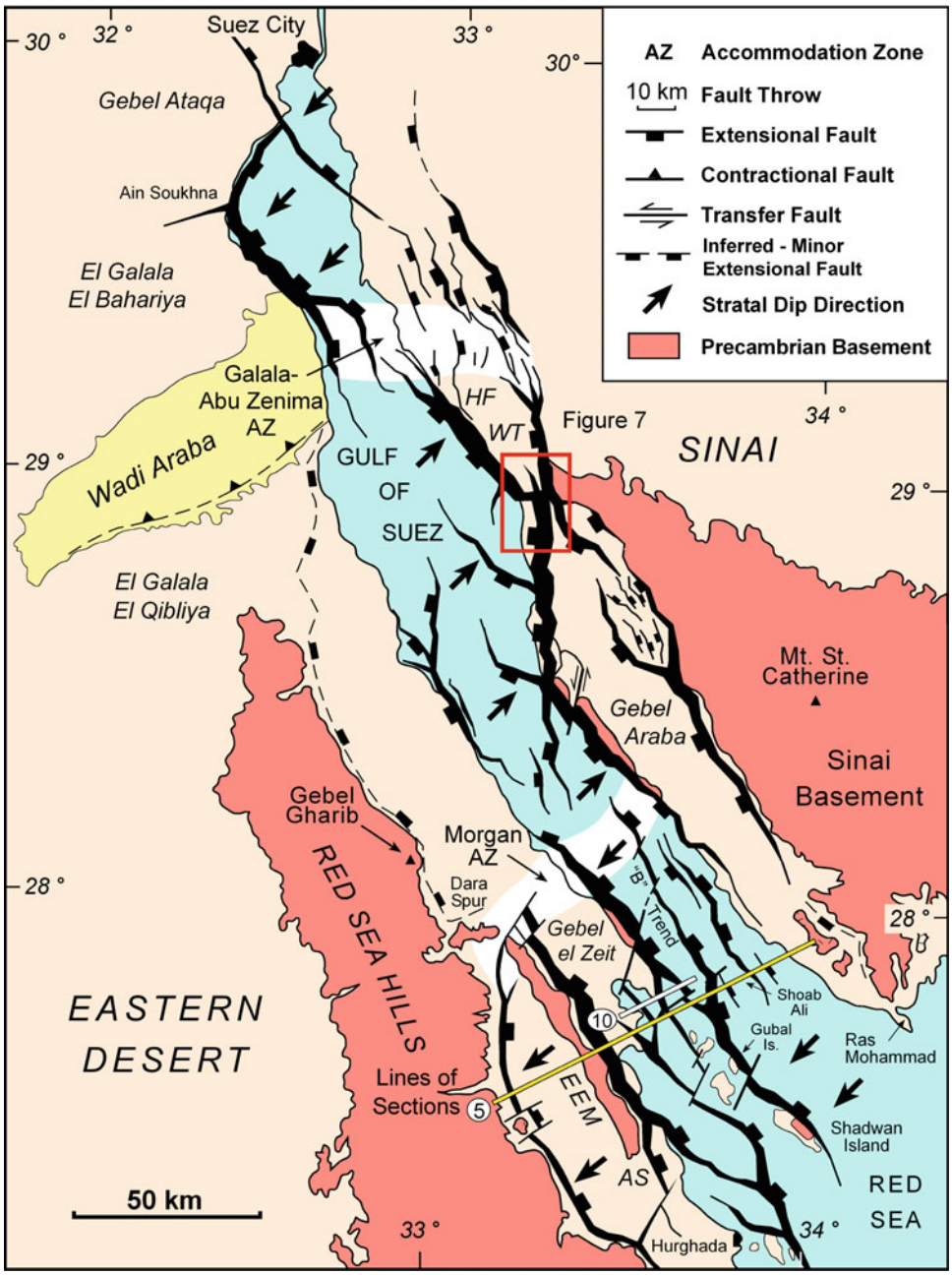

Fig. 4 Structure of the Gulf of Suez continental rift basin thought to be representative of the early structure of the Red Sea (after Khalil 1998; Bosworth and McClay 2001). *AS* Abu Shaar el Qibli, *EEM* Esh el Mellaha basement range and SW-dipping basin, *HF* Hammam Faraun fault block

northern Red Sea was remarkably similar to that of the Gulf of Suez. This confirmed the idea that the heavily explored—there are now nearly 4,000 wells drilled—and well-exposed Gulf of Suez could be utilized as an analogue for the early structural and sedimentologic history of the northern Red Sea.

On a regional scale, the Gulf of Suez consists of three sub-basins, each ~100 km in length and ~50–90 km in width (Fig. 4). Internally, each of these sub-basins consists of nested, rotated fault blocks (Fig. 5). Structural complexity and degree of stratal rotation increase systematically toward the south (Colleta et al. 1988; Patton et al. 1994). Moustafa (1976) analyzed available dipmeter and other subsurface data and recognized that within each sub-basin, the regional dip of beds is consistently in one direction, and hence, the overall geometry is that of a large-scale half graben broken up into a series of smaller half grabens. In the southern sub-basin, dip is generally to the southwest; in the central sub-basin, to the northeast; and in the northern sub-basin, again to the southwest. Hence, the "polarity" of the basins flips back and forth along the rift axis in what Moustafa referred to as dip domains. Similar large-scale reversals in structural dip, or major offsets of sub-basins with similar dip, have been identified in most continental rifts. The boundaries between these sub-basins have been named accommodation

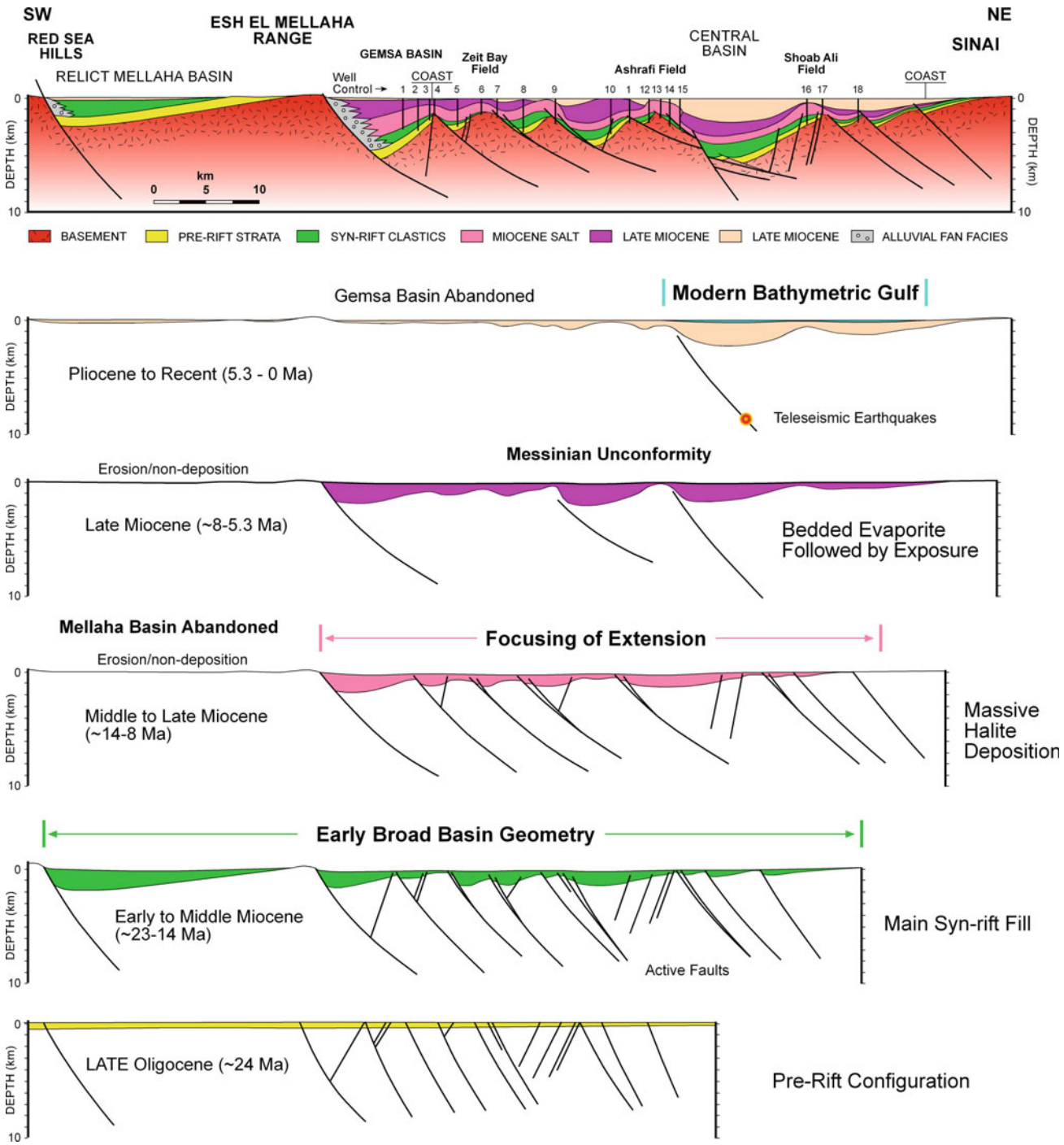

Fig. 5 Structural cross section of the southern Gulf of Suez and sequential views of sediment accumulation and sites of active faulting (after Bosworth 1994, 1995). Location is shown in Fig. 4

zones (Bosworth 1985; Rosendahl et al. 1986) or transfer zones (Morley et al. 1990; Moustafa 1997). In my original discussion of these common features, it was specifically noted that I was referring to crustal-scale sub-basin boundaries; there are smaller structures in most rifts that are better described as transfer faults (Gibbs 1984) or relay ramps (Larsen 1988; Peacock and Sanderson 1991).

The alternating half-graben geometry theme is not restricted to the Gulf of Suez. Along the Red Sea margin of Egypt, another polarity reversal has been recognized in outcrop in the vicinity of Quseir (Fig. 6; Jarrige et al. 1990; Younes and McClay 2002; Khalil and McClay 2009). North of the Quseir accommodation zone, structural dip is to the southwest and represents a regional continuation of the

Fig. 6 Principal structural features of the Quseir–Duba accommodation zone after restoring the Egyptian and Saudi Arabian margins to a pre-rift configuration at circa 23 Ma [restoration from Bosworth and Burke (2005); Africa is held stationary in this view with present-day north to the top]. Late Neoproterozoic Najd shear zones are shown as *blue dashed lines* [Egyptian terminology is from Khalil and McClay (2009)]. Miocene extensional faults are shown in *red* or *yellow* depending on direction of dip. Faults are plotted on SPOT imagery on the Egyptian margin and QuickBird imagery on the Saudi margin courtesy of Google Earth

southern Gulf of Suez sub-basin. At Gebel Duwi, the structural dip changes to the northeast. On the Saudi margin, the same structural change occurs south of Duba. After restoring the Red Sea to an Early Miocene configuration (see below), the Gebel Duwi and Duba accommodation zones are linked and pass through the area of the Brothers Islands (Bosworth 1994; Bosworth and Burke 2005). Fantozzi and Sgavetti (1998) recognized the presence of accommodation zones in outcrops along the paired margins of the Gulf of Aden, so this can reasonably be interpreted to have been a general attribute of the entire Red Sea–Gulf of Aden continental rift system.

At the scale of individual fault blocks, the Gulf of Suez and northern Red Sea margins display a great variety of sizes and styles of structuring (Angelier 1985; Jarrige et al. 1986; Colletta et al. 1988; Moretti and Colletta 1988; Perry and Schamel 1990; Bosworth 1995). The largest fault blocks are generally positioned on the outboard margins of the basin, as at Esh el Mellaha in the Gulf of Suez which has a length of 80 km and a width of 25 km (Fig. 4). The syn-rift stratigraphy present on these large blocks is typically only that produced during the earliest phase of extension, and then, their bounding faults ceased moving and the sub-basins were abandoned (Fig. 5). These "relict basins" (Bosworth 1994) are present along both sides of the Gulf of Suez and the northern Red Sea (Szymanski 2013). Stratal rotation in the relict basins is typically only 10–20°. More interior to the rift, fault block dimensions are smaller, the amount of rotation typically systematically increases toward the rift axis, and the movement on faults continued longer into the syn-rift history. Stratal dip along the axis of the southern Gulf of Suez locally exceeds 50° (Bosworth 1995).

In outcrop, vertical fault geometry is generally difficult to constrain—exposures of fault planes are simply too limited, except in rare cases of extreme topography. Both interpretations of basement-involved listric, detached faulting and bookshelf or domino-style faulting have been presented for many parts of the Red Sea and Gulf of Suez (Davison et al. 1994; Geoffroy et al. 1998; Perry and Schamel 1990; McClay et al. 1998). In some oil fields in the southern Gulf of Suez, basement faults have been penetrated by multiple wellbores. Some of these fault planes display abrupt changes in dip with depth, and others are most simply interpreted as listric in profile (Bosworth 1995; Bosworth et al. 2012). Correctly interpreting fault geometry is critical to estimates of horizontal extension and also for proper placement of exploration and development wells.

Along-strike fault geometry is much better documented in most exposed rift settings, and this is certainly the case in the Gulf of Suez and Red Sea. Surface traces of many of the larger extensional faults show a characteristic zigzag pattern, particularly where the footwall block is crystalline basement (Fig. 6; Jarrige et al. 1986; McClay et al. 1998). In some cases, subsurface data (wells, seismic) suggest that this is partly erosion of fault line scarps along pre-existing basement fractures and faults. However, many of the angular changes in strike are real and represent intersection of the predominantly NW–SE to NNW–SSE striking extensional faults with hard-linkage transfer faults/cross-faults of a variety of orientations. In the Gulf of Suez, the largest cross-faults are ~NNE–SSW and are important both on Sinai and in the Eastern Desert (Bosworth 1995; Bosworth et al. 1998; McClay et al. 1998). NE–SW striking cross-faults, perpendicular to the extensional faults, are often present in subsurface interpretations but are generally less important in outcrop. In the northern Red Sea, Neoproterozoic WNW–ESE striking Najd shear zones play the most significant role in modifying Miocene fault geometry (Figs. 3b, 6; Younes and McClay 2002; Khalil and McClay 2009).

Stratigraphy

The age and distribution of the pre-Red Sea stratigraphy of the Arabian Peninsula and northeast Africa have been extensively documented from outcrop studies and in the subsurface of the Gulf of Suez (Beydoun 1978; Hadley and Schimdt 1980; Klitzsch 1990; Schandelmeier and Reynolds 1997; Issawi et al. 1999; Ziegler 2001, reviewed in Bosworth et al. 2005; Guiraud et al. 2005). However, none of the offshore wells drilled in the Red Sea has penetrated any definitive Paleozoic or Mesozoic section (except immediately at the Sudanese coastline; Bunter and Abdel Magid 1989). Only at Zabargad Island (Fig. 1) is there exposed ~200 m of marine strata, dated as Early Cretaceous in age (Bosworth et al. 1996). As the richest source rocks in the Gulf of Suez are pre-rift limestones, the lack of pre-rift Red Sea sedimentary rocks has always been considered a major exploration risk in this basin (Beydoun 1989; Beydoun and Sikander 1992).

The thickness of the pre-Red Sea stratigraphic section increases both toward the far north and south (see Bosworth et al. 2005 their Fig.9). In Egypt, this is due to the large wedge of sedimentary rock developed south of Paleo- and Neotethys; in Eritrea, it is related especially to a thick Jurassic section associated with the opening of the Indian Ocean. In both areas, the pre-rift stratigraphy reaches about 2,500 m in total.

The literature on the syn-rift stratigraphy of the Red Sea is also voluminous. Unlike the pre-rift strata, the offshore Red Sea has provided a wealth of information from the few wellbores that have been drilled, particularly with regard to the age of the stratigraphic units. This has been reviewed by Tewfik and Ayyad (1984), Barakat and Miller (1984), Miller and Barakat (1988), Bunter and Abdel Magid (1989), Hughes and Beydoun (1992), Coleman (1993), Hughes and Filatoff (1995), Hughes et al. (1999), and Hughes and Johnson (2005). The closely related stratigraphy of the Gulf of Suez is summarized in Evans (1988), Richardson and Arthur (1988), Hughes et al. (1992), Patton et al. (1994), Wescott et al. (1997), McClay et al. (1998), Plaziat et al. (1998), and Bosworth and McClay (2001).

The base of the syn-rift section includes heterogeneous and laterally discontinuous beds of sandstone and conglomerate in most parts of the rift system (Fig. 7). The basal beds locally contain clasts of basalt or interdigitations of basalt flows or pyroclastics (e.g., Hadley et al. 1982; Schmidt et al. 1983; Sellwood and Netherwood 1984). The depositional environments include lacustrine and fluvial to marginal marine. In offshore Eritrea, this section has been dated as late Chattian, ~27.5–23.0 Ma (Hughes et al. 1991). Further north along the Saudi and Sudanese margins and into the Gulf of Suez, the oldest strata that are definitively syn-rift are Aquitanian in age, ~23.0–20.4 Ma (data reviewed in Bosworth et al. 2005). The top of this rift initiation package often contains shallow marine limestone and thin evaporite beds (Saoudi and Khalil 1986; Evans 1988; Bosworth et al. 1998).

The transition into the main phase of syn-rift sedimentation is diachronous between some individual fault blocks but regionally occurs at the base of the Burdigalian at ~20.4 Ma. This corresponds to when the fission track data indicate the presence of a well-established and rapidly rising rift shoulder and supports a thermomechanical linkage between extension-driven subsidence and flank uplift (Steckler 1985; Joffe and Garfunkel 1987; Steckler et al. 1988). Subsidence rates increased dramatically, with up to 1,500 m of open marine Globigerina-bearing shale and marl and turbiditic sandstone deposited in axial sub-basins (Fig. 9a). In the Gulf of Suez, the Burdigalian marls often contain total organic carbon (TOC) of 1.5–2.2 % and constitute an important hydrocarbon source rock (Alsharhan 2003). This may also be the case in the Red Sea, but the distribution of appropriate facies is not well constrained (Beydoun 1989). TOC measured in wells along the Egyptian Red Sea margin is 0.67–1.14 % (Barakat and Miller 1984) and would not be considered a significant source rock by most petroleum geologists.

The Burdigalian Red Sea and Gulf of Suez sections also contain thick sandstone facies that constitute important reservoir objectives. This is the case for the two largest known fields, Morgan and Belayim in the central Gulf (Egyptian General Petroleum Corporation 1996). The depositional environments of the sandstones are submarine fan and channel complexes in the basin axes that are thought to have been sourced from structurally controlled point sources

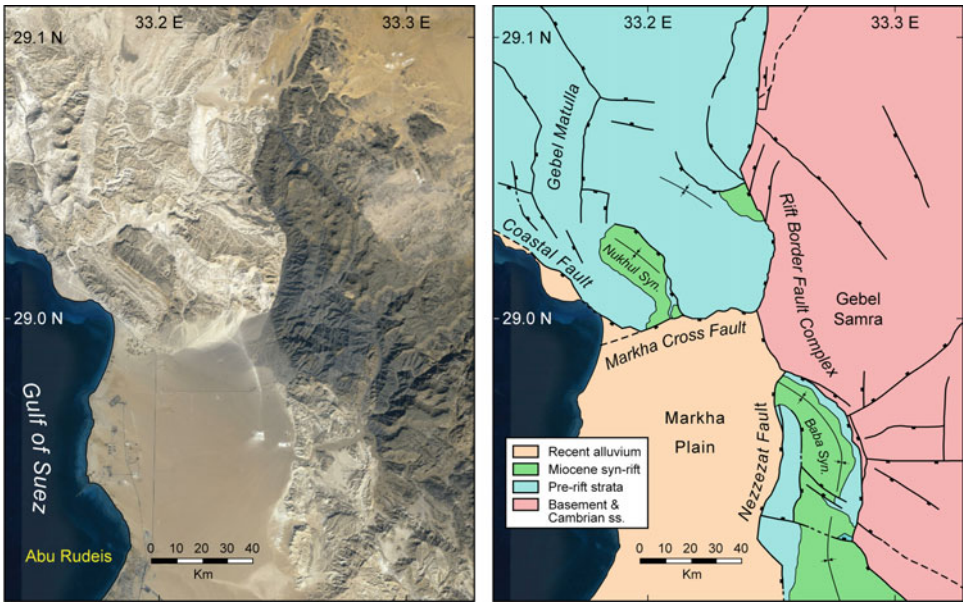

Fig. 7 High-resolution QuickBird satellite image of part of the border fault complex of the central Gulf of Suez (*image* acquired and processed for Apache Corporation by Spatial Energy). Outcrop geology is simplified from Khalil (1998) and Bosworth et al. (2012). Location is shown in Fig. 4. *Syn.* syncline. Transverse Mercator projection

along the basin margins (Lambiase and Bosworth 1995; Wescott et al. 1997; Khalil and McClay 2009). In more proximal fault blocks, the Burdigalian section often contains conglomerates and sandstones deposited as alluvial fans and fan deltas (Fig. 8b; Sharp et al. 2000; Young et al. 2000).

The main syn-rift fill continued into the early Middle Miocene (Langhian) and a second brief period of evaporite deposition occurred throughout most of the rift system (Fig. 8). Deep marine conditions then reappeared but were short lived as nearly the entire basin began depositing evaporites at about 14 Ma (early Serravallian). The principal evaporite minerals are halite and anhydrite/gypsum, and these are interbedded with conglomerate, sandstone, and shale depending on the position within the various sub-basins. Another brief period of normal marine deposition returned in the late Serravallian during which extensive carbonate platforms were developed (Fig. 9c; Bosworth et al. 1998; Cross et al. 1998). The Late Miocene was typified throughout by restricted marine evaporite deposition and interbedded conglomerate, sandstone, and shale similar to the early Serravalian.

Within salt walls and domes, the massive halite sections sometimes exceed 3 km thickness. Age control within the various evaporite-dominated formations is rare, but the uppermost shale interbeds have yielded broad ranging "Late" Miocene ostracods and calcareous nannoplankton (El-Shafy 1992). These beds are capped by an unconformity that extends throughout the Gulf of Suez and Red Sea which is in turn overlain by Pliocene strata. This unconformity—the "S" reflector of Ross et al. (1973) and the "top Zeit" of industry parlance—is therefore essentially equivalent to the Messinian unconformity of the Mediterranean (Coleman 1993). Like the Mediterranean, the Red Sea must have been mostly a dry basin during the Late Messinian.

Salt Flowage

The formation of salt domes and walls has been studied in both the subsurface and along the margins of the Red Sea and Gulf of Suez (Hassan and Dashlouty 1970; Ross and Schlee 1973; Mulder et al. 1975; Khedr 1984; Miller and Barakat 1988; Patton et al. 1994; Bosworth 1995; Heaton et al. 1995; Bosence et al. 1998, reviewed in Orszag-Sperber et al. 1998). Both local salt overhangs and larger salt canopies have been described (Fig. 10). Consensus is that flowage of the Middle to Late Miocene massive halite began soon after its deposition and subsequently impacted the distribution of younger sediments. In general, the configuration of the salt walls in the Gulf of Suez follows that of the underlying extensional fault blocks and hard-linkage transfer faults (Bosworth 1995).

In many oil fields in the Gulf of Suez, the ultimate top seal is the massive salt, and hence, mapping this surface is a key aspect of exploration. As in other salt basins, the high seismic velocities of the evaporites and their complex geometry make imaging the sub-salt structure and stratigraphy exceptionally difficult. Some progress in addressing this issue has been reported in recent years (Mougenot and Al-Shakhis 1999; Musser et al. 2012).

Volcanicity

The volcanic rocks of the Red Sea basin provide critical information about the timing of rifting, the nature of the subcrustal mantle, the possible connections between the Afar plume and rifting, the transition from continental to oceanic rifting, and the onset of seafloor spreading. Coleman (1993)

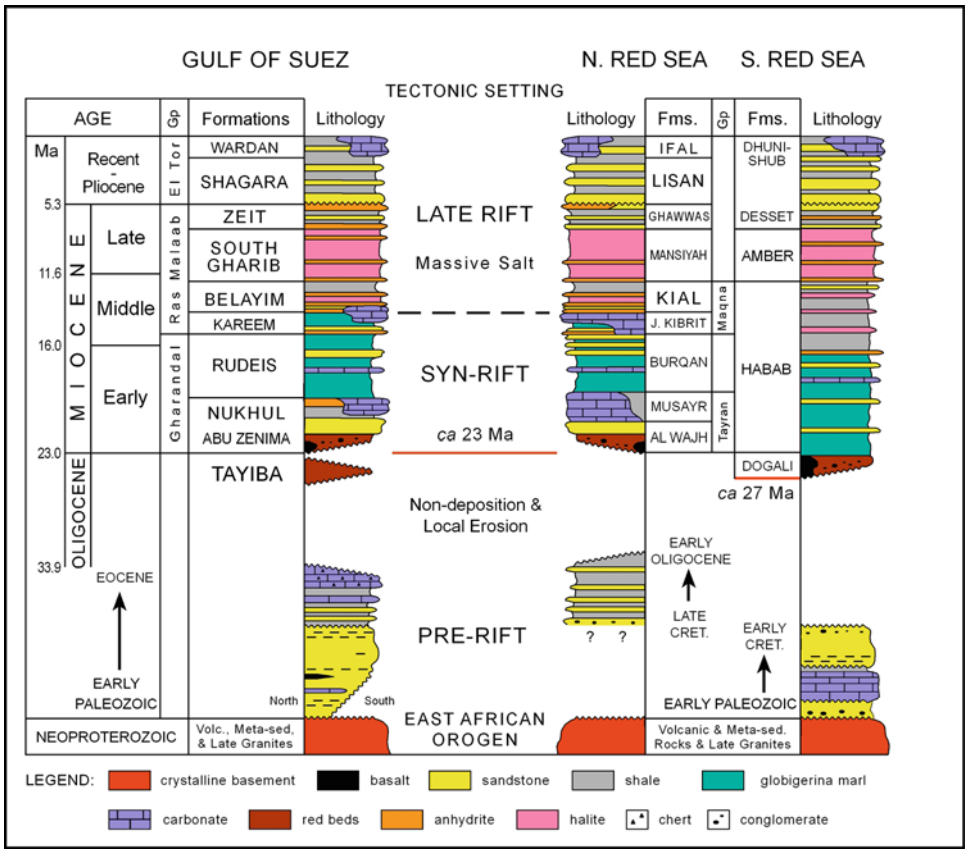

Fig. 8 Simplified stratigraphic sections and terminology of the Gulf of Suez and Red Sea (after Bosworth and Burke 2005 and references therein). Timescale is from Gradstein et al. (2004)

has provided a thorough introduction to this material, and a recent review is provided by Szymanski (2013). In terms of chronology, volcanism can be discussed in four phases: (1) the Afar and Yemen trap basalts and Older Harrats; (2) sheeted dike complexes of the Saudi Arabian margin and time-equivalent isolated dikes and flows of Sinai and northern Egypt; (3) the Younger Harrats; and (4) post-Miocene volcanism of the Red Sea axial trough.

$^{40}Ar/^{39}Ar$ age dating has shown that eruption of the Afar basalts/trachytes began at 31 Ma, followed by rhyolitic eruptions ~1 Ma later and then a period of ~5 Ma of much more subdued outflowings of basalts and ignimbrites (Zumbo et al. 1995; Rochette et al. 1997; Chernet et al. 1998; George et al. 1998; Ukstins et al. 2002; and Coulié et al. 2003). Smaller occurrences of rhyolites on the southern Sudanese margin were similarly dated at 30 Ma (Kenea et al. 2001) and basalts at the Older Harrat Hadan 28–26 Ma (Sebai et al. 1991; Féraud et al. 1991). The Yemeni traps show the same sequence as Afar, with basalts beginning at 31 Ma followed by massive ignimbrites from 30 to 26 Ma (Baker et al. 1994, 1996; Ukstins et al. 2002; Coulié et al. 2003).

The second phase of Red Sea volcanism principally involved intrusion of NW–SE striking basaltic dikes along the Yemen and Saudi Red Sea margins, Sinai, and northern Egypt. In southern Saudi Arabia, the dikes are exposed with coeval layered gabbro and granophyre (McGuire and Coleman 1986; Coleman 1993). The dikes in Saudi Arabia were intruded over a brief time span from ~24 to 22 Ma (Table 1; Sebai et al. 1991). Basaltic dikes in Sinai and the vicinity of Cairo correspond to the same ages and fed an area of flows that covered ~15,000 km^2 (preserved) to perhaps 25,000 km^2 (original) (Figs. 11 and 12). Though authors differ on the interpretation of the Cairo basalts, field relationships suggest that they were erupted more or less as a single geologic event similar to the initial basaltic volcanism at Afar (Bosworth et al. 2015) and can be thought of as a short-lived "mini-plume." Recent analyses of trace elements and Sr–Nd–Pb–Hf isotopes suggest that these sub-alkaline basalts were derived from mixing of an Afar plume-like source with metasomatized continental lithosphere (Endress et al. 2011). In the Gulf of Suez, the circa 23 Ma basalts are found associated with the very basal syn-rift sedimentary units (Fig. 12a; Sellwood and Netherwood 1984; Bosworth and McClay 2001; Jackson 2008). The weighted mean average plateau and integrated total fusion ages for the Red Sea dikes and flows of Egypt are 23.0 ± 0.1 and 22.8 ± 0.1 Ma, respectively (Table 1), essentially at the Oligocene–Miocene transition (Gradstein et al. 2004). The weighted mean average of Sebai et al.'s dates for Saudi Arabia is slightly younger at 21.8 ± 0.03 Ma, but these

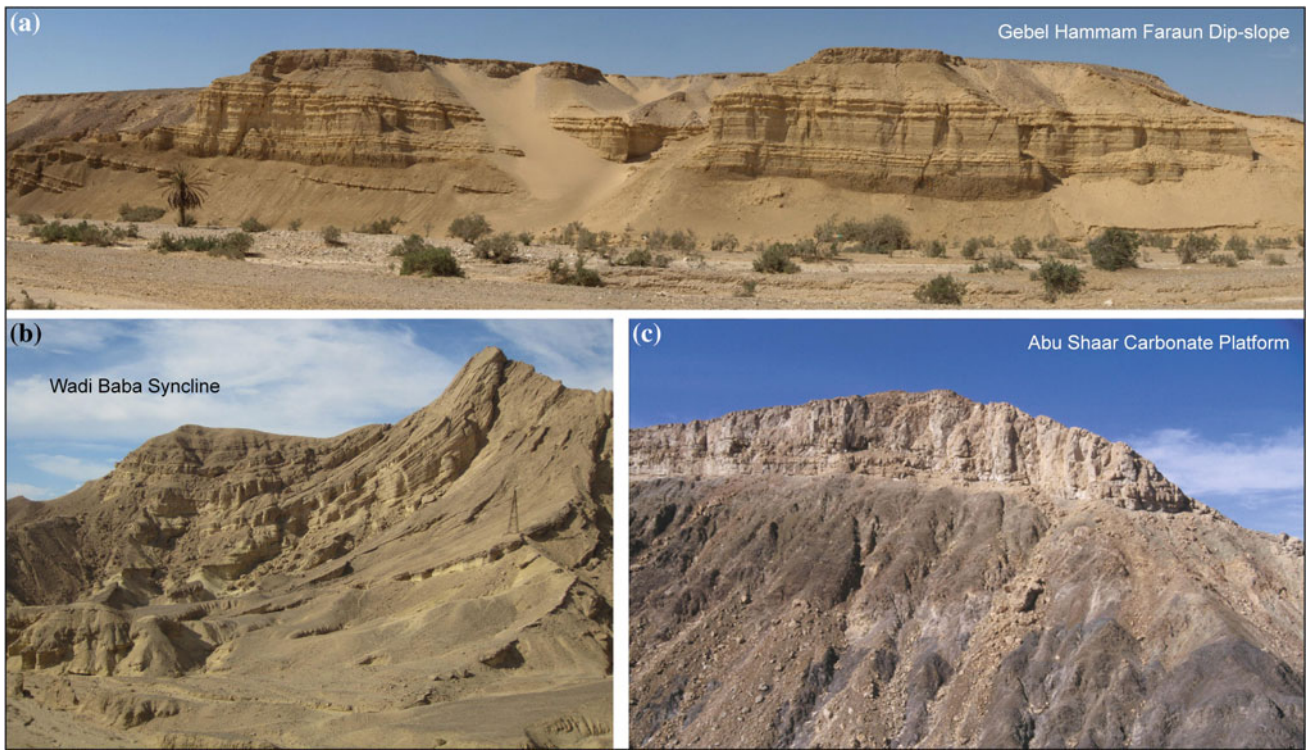

Fig. 9 Field photographs of syn-rift strata from the northern Red Sea rift system (Egypt). **a** Early Miocene Rudeis Formation shale and thin sandstone, the main syn-rift fill facies of the basin. From the dip slope of the Hammam Faraun fault block (Fig. 4); **b** proximal fan-delta sandstone and conglomerate near the rift border fault complex and deformed by a syn-rift fault propagation fold at Wadi Baba (Fig. 7); **c** Middle Miocene reef platform and carbonate talus overlying crystalline basement at Abu Shaar el Qibli northwest of Hurghada (Fig. 4). These carbonate rocks are time stratigraphic equivalents of the Belayim Formation of Fig. 8

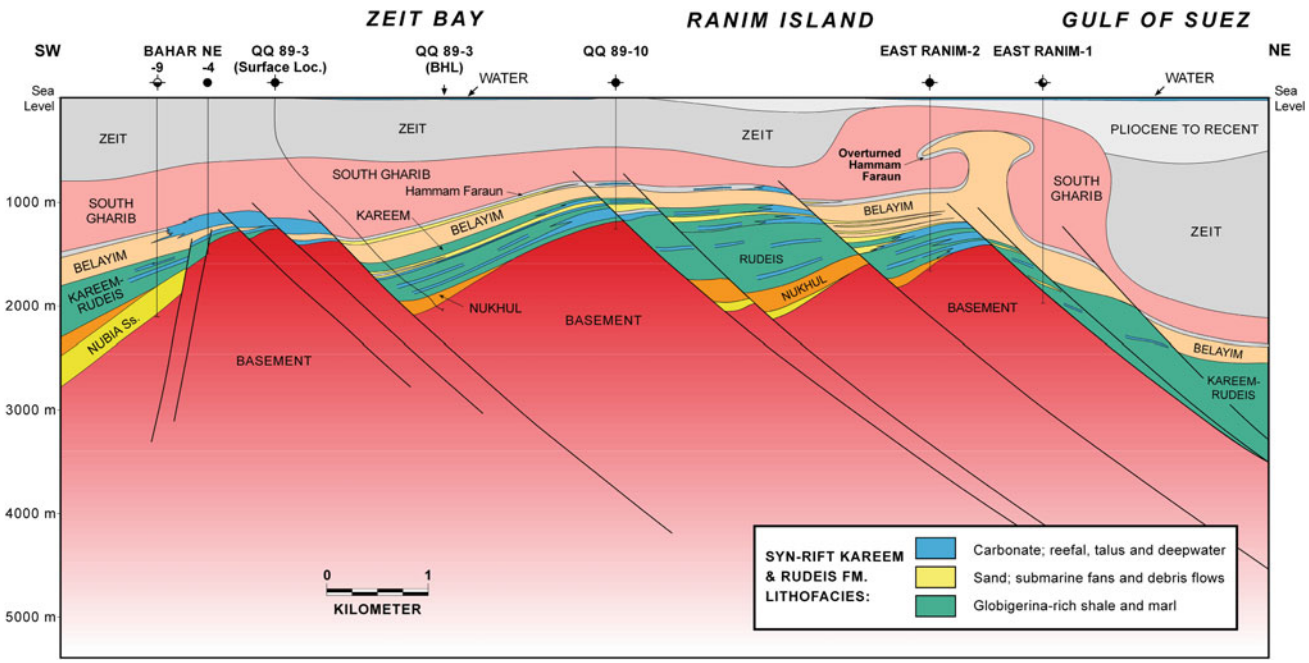

Fig. 10 Structural cross section of the salt ridge at East Ranim. The lithofacies of the main syn-rift Rudeis and Kareem Formations are shown by *color coding*. The South Gharib and Belayim Formations contain massive halite that has flowed to produce a classic *mushroom*-shaped structure with a salt overhang. East Ranim-2 penetrated the Hammam Faraun Member three times, once in an overturned orientation. Location is shown in Fig. 4

Table 1 Compilation of Ar^{40}/Ar^{39} data for the Red Sea dike event at the Oligocene–Miocene boundary

Location		Outcrop	Sample Name	Mineral	Weighted mean plateau age	Integrated total fusion age	Source
Country							
North	Egypt	Cairo		Whole rock	22.4[a]		Lotfy et al. (1995)
		Cairo		Whole rock	22.6[a]		Lotfy et al. (1995)
		Gebel Qatrani		Whole rock	23.67 ± 0.15		Kappelman et al. (1992)
		Gebel Qetrani		Whole rock	23.68 ± 0.14		Kappelman et al. (1992)
		Gebel Qatrani		Whole rock	23.62 ± 0.16		Kappelman et al. (1992)
		Gebel Qetreni	*08-GQ-01*	Whole rock	21.7 ± 0.3	22.0 ± 0.8	Bosworth et al. (2015)
		Gebel Gatrani	*08-GQ-02*	Whole rock	21.4 ± 0.3	20.0 ± 0.3	Bosworth et al. (2015)
		Gebal Qatrani	*08-GQ-03*	Whole rock	23.2 ± 0.4	24.0 ± 0.8	Bosworth et al. (2015)
		West Faiyum	*WFAY-1*	Whole rock	23.5 ± 0.7	24.0 ± 0.5	Bosworth et al. (2015)
		West Faiyum	*WFAY-2*	Whole rock	22.1 ± 0.4	21.7 ± 0.6	Bosworth et al. (2015)
		Bahariya Oasis	*09-WD-01*	Whole rock	23.1 ± 0.2	22.9 ± 0.2	Bosworth et al. (2015)
		Bahariya Oasis	*09-WD-02*	Whole rock	23.6 ± 0.2	23.2 ± 0.2	Bosworth et al. (2015)
		Bahariya Oasis	*09-WD-03*	Whole rock		20.8 ± 0.2	Bosworth et al. (2015)
		Bahariya Oasis	*09-WD-04a*	Whole rock		24.2 ± 0.2	Bosworth et al. (2015)
		Bahariya Oasis	*09-WD-04b*	Whole rock		25.0 ± 0.3	Bosworth et al. (2015)
		Qaret Dab'a	*09-WD-05*	Whole rock	23.4 ± 0.4	23.1 ± 0.4	Bosworth et al. (2015)
		Wadi Tayiba	*06-GZ-02*	Whole rock		23.1 ± 0.9	Bosworth et al. (2015)
		Wadi Nukhul	*06-GZ-03*	Whole rock	24.4 ± 0.3	23.0 ± 3.0	Bosworth et al. (2015)
		Weighted mean average			23 0 ± 0 1	22.8 ± 0.1	
South	Saudi Arabia	Al Wajh	*89A53*	Plagioclase	22.50 ± 0.06		Sebai et al. (1991)
		AI Lith	*88AR1*	Plagioclase	22.3 ± 0.6		Sebai et al. (1991)
		Al Lith	*AS82*	Plagioclase	23.3 ± 0.5		Sebai et al. (1991)
		Al Lith	*88A4*	Amphibole	24.0 ± 0.2		Sebai et al. (1991)
		AI Lith	*88AR67*	Plagioclase	21.1 ± 0.2		Sebai et al. (1991)
		AI Lith	*88AR69*	Plagioclase	21.5 ± 0.1		Sebai et al. (1991)
		AI Lith	*AS85*	Plagioclase	21.7 ± 0.3		Sebai et al. 1991
		AI Birk	*89A44*	Whole rock	23.9 ± 0.3		Sebai et al. (1991)
		AI Birk	*89A44*	Biotite	22.3 ± 0.5		Sebai et al. (1991)
		AI Birk	*88AR55*	Hornblende	21.1 ± 0.5		Sebai et al. (1991)
		AI Birk	*88AR53*	Hornblende	22.0 ± 0.3		Sebai et al. (1991)
		Tihama Asir	*88AR14*	Whole rock	21.8 ± 0 3		Sebai et al. (1991)
		Tihama Asir	*88AR48*	Plagioclase	24.5 ± 1.3		Sebai et al. (1991)
		Tihama Asir	*88AR43*	Plagioclase	22.6 ± 0.9		Sebai et al. (1991)
		Tihama Asir	*88AR8*	Plagioclase	21.25 ± 0.05		Sebai et al. (1991)
		Tihama Asir	*88AR37*	Plagioclase	22.0 ± 0.5		Sebai et al. (1991)
		Tihama Asir	*88AR35*	Plagioclase	22.2 ± 1.1		Sebai et al. (1991)
		Weighted mean average			21.8 ± 0.03		

[a] not used in weighted average as no standard deviation provided

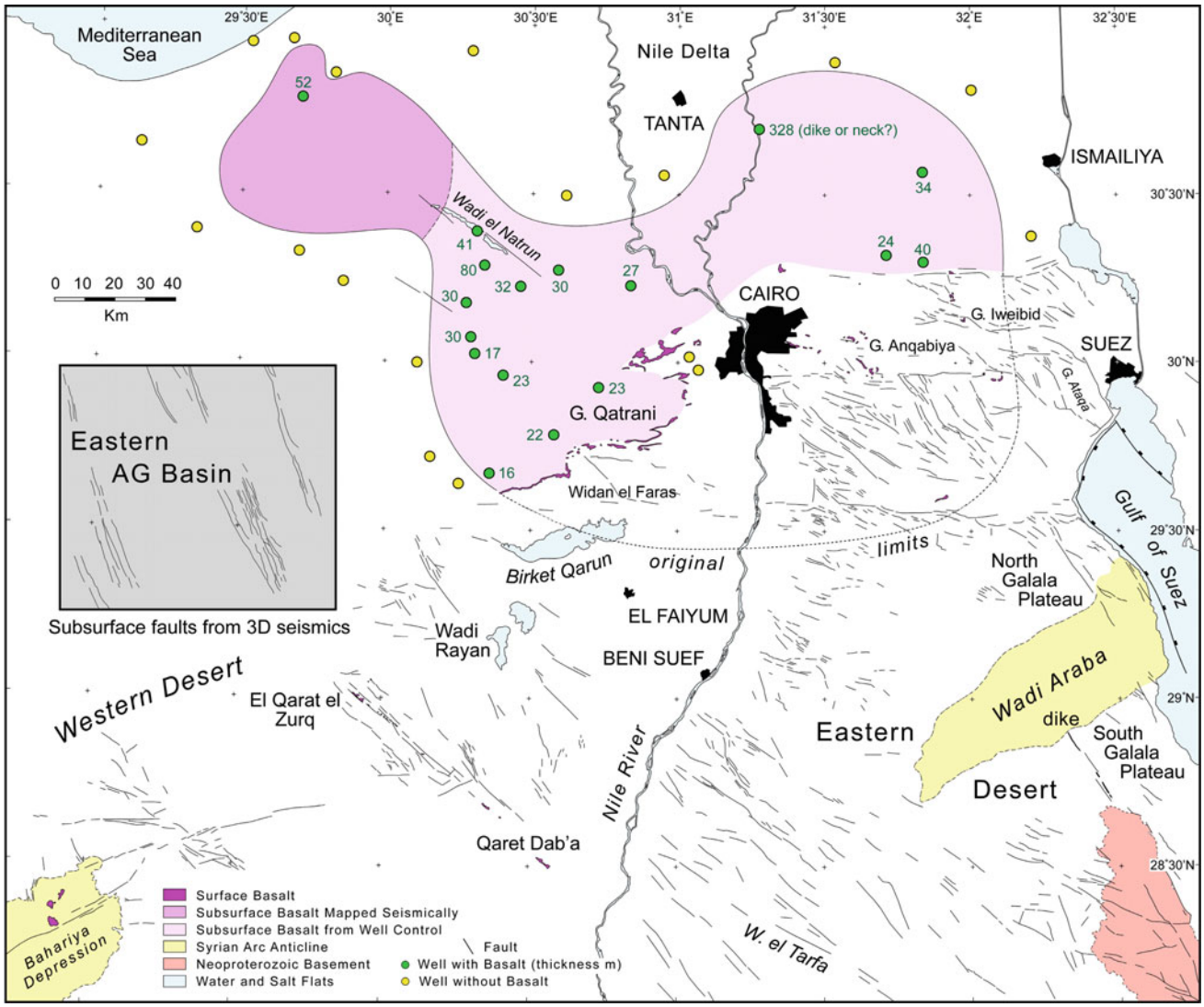

Fig. 11 Cairo basalt province and faulting associated with the northern limits of the greater Red Sea rift system. The *purple shaded* region shows the extent of 23–22 Ma basalt flows in the subsurface, with an area of approximately 15,000 km^2 (would have covered 20,000–25,000 km^2 prior to erosion). Darker shading is the area of flows mapped by Williams and Small (1984) in 2D reflection seismic data. Lighter shading is the area of flows based solely on well penetrations (thickness of flow is annotated). *Gray shaded box* shows basal Miocene-age subsurface faults in a merge of several large-scale 3D seismic surveys. After Bosworth et al. (2015). Transverse Mercator projection

basalts were emplaced over a much greater area, and this average may include several closely related eruptive events. The age of the onset of dike intrusion was statistically the same in both the Gulf of Suez and Saudi margin.

After the 24–22 Ma dike event, volcanism ceased in most parts of the Red Sea basin. Exceptions are Afar, where a complex igneous history continued to the present day (Barberi et al. 1972; Varet 1978; Zanettin et al. 1978; Berhe 1986; Vellutini 1990; Tefera et al. 1996), and Harrat Ishara (north of Madinah) which experienced basaltic volcanism from ~17 to 14.5 Ma (Szymanski 2013). In the Middle Miocene, volcanism returned to far-reaching areas of the Arabian Peninsula: Harrat ash Shaam, Jordan at ~13 Ma (Ilani et al. 2001), and the Younger Harrats of Saudi Arabia —Uwayrid ~12 Ma, Khaybar ~11 Ma, and Rahat ~10 Ma (Coleman et al. 1983; Coleman 1993 and references therein). Volcanism continues to the Recent in these and other Younger Harrats, often with north–south aligned vents and dikes. These orientations support the interpretation that in the Arabian shield, the maximum horizontal stress has been north–south during post-Miocene times (Bosworth and Strecker 1997). This contrasts with the central platform areas of Arabia (Ghawar province) where the maximum horizontal stress is presently ENE–WSW (Ameen 2014).

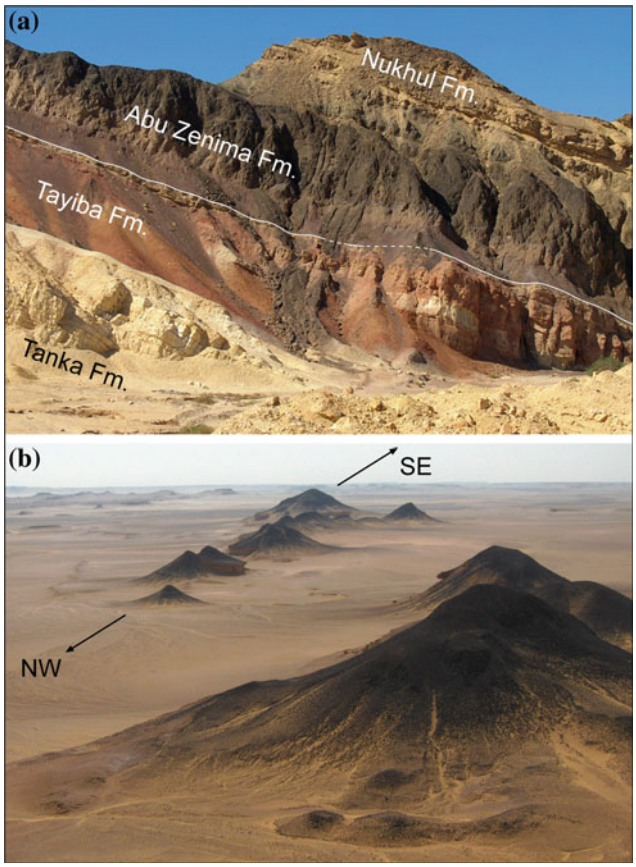

Fig. 12 Field photographs of circa 23 Ma basaltic volcanism associated with rift initiation in the northern Red Sea rift system. **a** Basalt flow within the Abu Zenima Formation at Wadi Tayiba in the northern Gulf of Suez (Fig. 4) overlain by Early Miocene Nukhul Formation syn-rift siliciclastic rocks; underlain by Oligocene Tayiba Formation pre-rift red beds and Late Eocene Tanka Formation white limestone. Base-rift unconformity is shown by white line; **b** NW–SE aligned monogenetic volcanic cones southwest of Faiyum in the Western Desert of Egypt (part of Qarat el Zurq–Qaret Dab'a trend in Fig. 11)

Typical mid-ocean ridge basalts (MORBs) of the Red Sea rift axis have been observed and sampled in situ by submersible dives (Monin et al. 1982; Juteau et al. 1983), and closely related tholeiites are exposed subaerially at the active axial shield volcano of Jabal at Tair Island in the very southern Yemeni Red Sea (Mattash 2008). The ongoing volcanism of the Red Sea axial trough is discussed in detail in other chapters of this book.

Lithospheric and Crustal Structure

Geophysical studies of the Red Sea have been reviewed by Cochran (2005), Cochran and Karner (2007), and Lazar et al. (2012). Gravity observations initiated with the coastal survey of von Triulzi (1898) and then the shipboard expedition of Vening Meinesz (1934). These data led to the fundamental observation that the Red Sea displays positive gravity anomalies that Girdler (1958) attributed to mafic intrusions into the basement complex. This can be thought of as the seed from which the concept that the Red Sea is undergoing oceanic spreading evolved (Lazar et al. 2012). Maximum Bouguer values exceed 100 mGal and are located along the median trough (Allan et al. 1964; Allan 1970; Makris et al. 1991a). In the southern Red Sea, the anomalies display a simple, approximately parallel relationship to the present-day coastlines. North of Zabargad Island, however, the anomalies are less continuous and trend more northwest than the coastlines (Cochran and Karner 2007). The northern Red Sea gravity anomalies have been interpreted as the expression of large, rotated fault blocks of continental crust (Martinez and Cochran 1988; Cochran and Karner 2007). Cochran (2005) inferred that the fault block arrays were segmented and separated by accommodation zones that trend normal to the coastlines. This configuration is very different than that proposed based on outcrop geology (Fig. 6; Bosworth 1994; Bosworth and Burke 2005), though the general concept of along-strike rift segmentation is in agreement.

Magnetic studies of the Red Sea followed the early gravity investigations (Allan et al. 1964; Drake and Girdler 1964). It was soon accepted that linear magnetic anomalies that are present on both sides of the axial deep in the southern Red Sea were produced by seafloor spreading (Allan 1970; Röser 1975; Searle and Ross 1975). The onset of spreading is thought to be ~5 Ma (Cochran 1983) at the Miocene–Pliocene transition and approximately coeval with the major Zeit unconformity discussed above. The magnetic character of the northern Red Sea is much more contentious. Anomalies there tend to be discrete, localized and normally magnetized (Cochran et al. 1986; Martinez and Cochran 1988; Guennoc et al. 1988), and therefore must have been produced within the past 780 ka (Brunhes chronozone) based on the geomagnetic polarity timescale (Shackleton et al. 1990; Gee and Kent 2007). These young features are interpreted to be individual volcanoes erupted within the northern axial deeps (e.g., Bannock and Shaban Deeps, Fig. 2b; Bonatti et al. 1984; Pautot et al. 1984) or localized intrusions. Martinez and Cochran (1988) similarly interpreted a sub-sea sediment piercing structure near the Brothers Islands to be a volcano built on the abyssal plain west of the axial trough. It has also been suggested that high-frequency, discontinuous but linear magnetic anomalies are present in the northern Red Sea dataset and that these were formed by seafloor spreading (Saleh et al. 2006).

Seismic refraction profiling has provided important constraints on the configuration of the Moho along the Red Sea margins of Egypt (Makris et al. 1981; Gaulier et al. 1988) and Saudi Arabia (Mooney et al. 1985; Prodehl 1985; Milkereit and Fluh 1985; Blank et al. 1986; Gettings et al.

1986). In the north, the un-thinned continental crustal thickness is ~40 km in both Arabia and Africa. At the coastlines, the crust has been thinned to ~20 km, though the limited data that are available suggest that the change is more abrupt on the Egyptian margin (see compilation in Voggenreiter et al. 1988). In southern Saudi Arabia, the 1,070 km US Geological Survey refraction line extends from the Farasan Islands to near Riyadh and has received a variety of interpretations. There is general agreement that the continental crust is ~38–45 km thick beneath the Arabian shield and that the Moho there is approximately horizontal. At the coastal plain, Mooney et al. (1985) interpreted an abrupt thinning of the crust to ~20 km and then further gradual tapering to less than 10 km thickness beneath the Farasan Islands. Prodehl (1985) modeled a much more gradual rise in the depth to the Moho starting west of the Asir Range and reaching ~14 km at Farasan. Milkeriet and Fluh (1985) interpreted abrupt thinning similar to Mooney et al. (1985) but with the presence of an intra-crustal high-velocity zone beneath the coastal plain. These various studies suggest that the crust along the shelf of the northern Red Sea is about 50 % of its original thickness and in the southern Red Sea (Saudi margin) about 25–30 %.

Early compilations of heat flow data demonstrated that the entire Red Sea basin is hotter than the worldwide average of ~60 mW/m^2 and that the magnitude of this anomaly increases toward the axial trough (Girdler 1970; Scheuch 1976; Girdler and Evans 1977). Heat flow along the margins of the northern Red Sea is typically about 125 mW/m^2 (Martinez and Cochran 1988), whereas in the Eastern Desert of Egypt, the average is slightly more than 70 mW/m^2 (Morgan et al. 1980). Along the Red Sea axis, values of 250–350 mW/m^2 are common with a maximum of ~400 mW/m^2 (Martinez and Cochran 1988; Makris et al. 1991b). The observed heat flow profiles have been modeled with respect to a variety of geometric and kinematic rift histories (simple shear, pure shear), and the general conclusions are that the zone of crustal thinning must have widened as extension initially progressed and then starting at ~5 Ma dramatically narrowed to a presently active width of ~20 km (Buck et al. 1988; Martinez and Cochran 1989). A simple shear lithospheric-scale detachment geometry (Wernicke 1985; Voggenreiter et al. 1988) could not reproduce the value or distribution of heat flow, and neither simple shear nor pure shear models resulted in shallow mantle melting. This suggested that an additional source of heat such as convection was required, in agreement with studies by McGuire and Bohannon (1989) of mantle zenoliths. These authors found that the temperature beneath western Arabia at a depth of 40 km is ~900 °C, much too high to be explained by the present measured shallow geothermal gradient. Hence, the postulated mantle upwelling must be very young, synchronous with Neogene rifting rather than prior, or there would have been time for equilibration of the shallow heat flow.

Plate Kinematics and Red Sea Restorations

Early models of the Red Sea basin as a pair of rifted continental margins focused on how much oceanic crust had been generated and resulted in two end members: (1) Young oceanic crust is restricted to the axial trough, and opening is therefore restricted to ~85 km (Girdler 1958; Drake and Girdler 1964; Hutchinson and Engels 1970, 1972; Lowell and Genik 1972; Ross and Schlee 1973) versus (2) the entire width of the Red Sea was formed by seafloor spreading and a pre-rift restoration should be coastline to coastline (McKenzie et al. 1970). Numerous intermediate models were subsequently developed (reviewed in Girdler and Whitmarsh 1974).

It was later generally accepted that oceanic spreading only started in the Red Sea about 5 Ma (discussed below), though continental rifting began in the Oligocene or Early Miocene. The early separation of Arabia from Africa therefore involved stretching of continental lithosphere or some other mechanism for generation of surface area, which needed to be incorporated in plate restorations (reviewed in Le Pichon and Francheteau 1978; Coleman 1993). Le Pichon and Francheteau (1978) interpreted the instantaneous pole of opening for the Red Sea from the magnetic lineaments of the southern axial trough and compared this with the total opening (Eulerian pole) of McKenzie et al. (1970) and key geologic constraints. They concluded that the movement of Arabia relative to Africa has been essentially stable since the Early Miocene, but that the total opening can only be on the order of 3°–4° rather than the 6° of McKenzie et al. Hence, they estimated total opening to be 150–200 km at 19°N latitude or about 65–115 km of nonspreading center-generated new surface. Numerous refinements and adjustments have been made to the LePichon and Francheteau and earlier reconstructions (Cochran 1983; Girdler and Underwood 1985; Bohannon 1986; Joffe and Garfunkel 1987).

GPS datasets for Arabia and adjacent plates are now very robust and indicate that Arabia is moving ~20.6 mm/yr north relative to a Eurasia-fixed reference frame (Fig. 1; ArRajehi et al. 2010). This agrees with larger scale plate circuit estimates for Arabia–Eurasia convergence for the past ~22 Ma (McQuarrie et al. 2003). Similarly, convergence between Africa (Nubia) and Eurasia of ~6.6 mm/yr has occurred for the past ~11 Ma. The agreement between geodetically derived, present-day instantaneous velocities, and plate tectonic, geologic-term velocities suggests that restoration of the Red Sea–Gulf of Aden rift system can be reasonably produced if an independent key basin parameter is known: either (a) time of rift initiation or (b) the starting

separation of some unchanged feature on both margins of the basin. ArRajehi et al. (2010) assumed coastline-to-coastline restoration (similar geometrically to McKenzie et al. but not necessarily all oceanic crust) and derived an age of initiation for Red Sea rifting of 24 ± 2.2 Ma. Detailed discussion of the significance of GPS results to Red Sea restorations is presented by Reilinger et al. in this volume.

Red Sea Rift Chronology

Continental Rifting

The initiation of continental rifting in the Red Sea is directly tied to the geologic history of Afar and the Gulf of Aden (reviewed in Bosworth et al. 2005 and references therein). Extension began in the eastern Gulf of Aden by ~30 Ma (late Early Oligocene), and the entire gulf was active by the mid-Oligocene though precise data are lacking (Fig. 13a; Roger et al. 1989; Hughes et al. 1991; Watchorn et al. 1998). In the southernmost Red Sea, offshore Eritrea, the base of the syn-rift section is dated as ~27.5 to ~23.0 Ma (Late Oligocene; Fig. 13b; Hughes et al. 1991). Similarly in the Afar region, major extension is interpreted to have begun by ~25 Ma (Fig. 13c; Barberi et al. 1972, 1975; Zanettin et al. 1978).

For the rest of the Red Sea, north as far as the Gulf of Suez and Cairo district of Egypt, definitive basal syn-rift strata are paleontologically dated to be ≤23 Ma (Early Miocene, Hughes and Beydoun 1992; Bosworth et al. 2005). As discussed above, these sedimentary rocks are interbedded with or contain detritus of basalts that are radiometrically dated 24–22 Ma (Table 1). Oligocene strata are locally present, the Tayiba Formation and lateral equivalents (Fig. 8). But these Oligocene red beds do not display a syn-tectonic relationship to Gulf of Suez faulting (e.g., Khalil 1998; Jackson et al. 2006; Jackson 2008). Recent paleontologic studies in western Sinai suggest that the base of the oldest syn-rift units is locally latest Oligocene (Hewaidy et al. 2012 reviewed in El Atfy et al. 2013). If correct, this is compatible with the uncertainty in the age of the basal basalts and the assertion that these basalts mark the onset of rifting. More paleontologic data for the southern Red Sea are needed, and better resolution within the "Late Oligocene" would be helpful, but it appears that continental extension invaded the entire Gulf of Aden and Afar region during the Early to Late Oligocene and then stalled briefly (perhaps 2–3 My). At the Oligocene–Miocene transition, dike intrusion and faulting shot from Eritrea to Egypt with no recognizable time difference—without discernible propagation (Fig. 13c; Richardson and Arthur 1988; Omar and Steckler 1995).

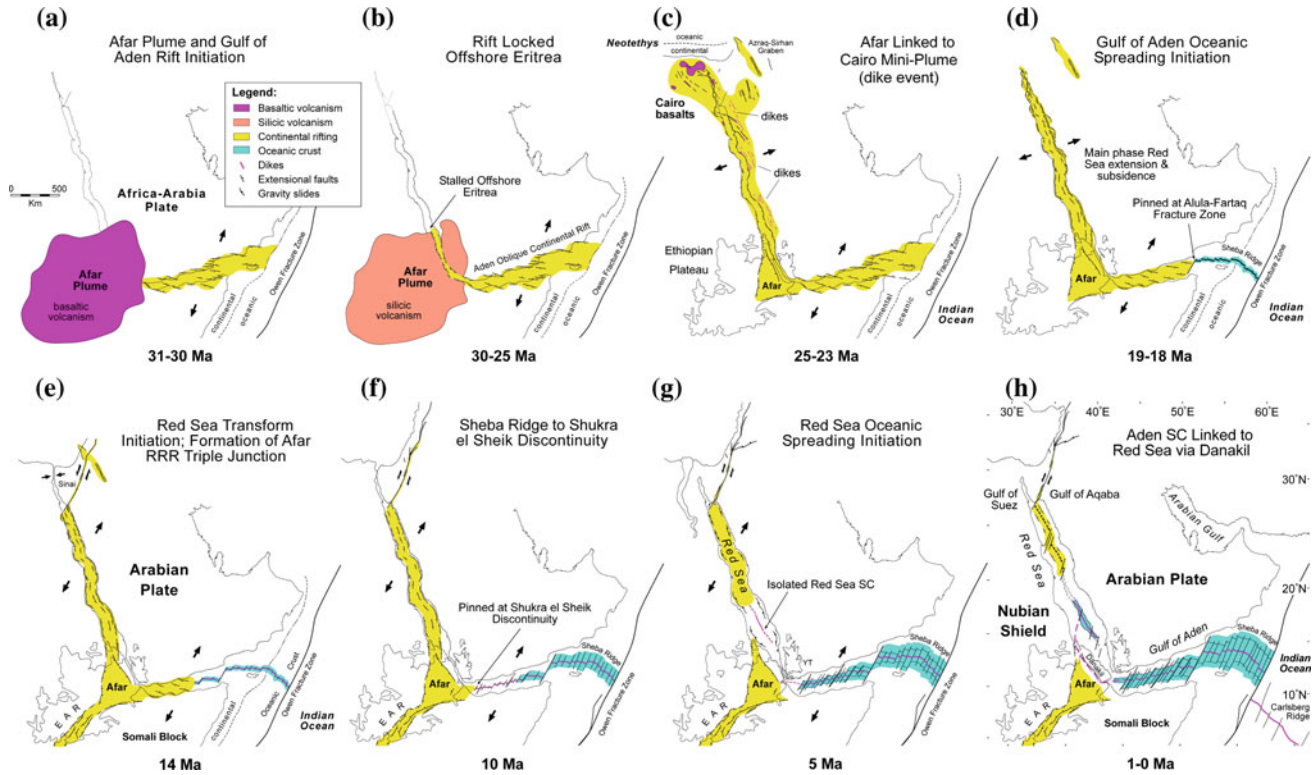

Fig. 13 Synthesis of continental and oceanic rift initiation and propagation in the greater Gulf of Aden–Red Sea rift system. Simplified from Bosworth et al. (2005). EAR = East African Rift; SC = spreading center

Where documented, the earliest syn-rift strata in the Gulf of Aden overlie marine pre-rift rocks of Oligocene or older age (Hughes et al. 1991; Robertson and Bamakhalif 1998; Bosworth et al. 2005). This suggests that this rift initiated near sea level. The evidence is not as definitive for the Afar region. A regional peneplain separates the pre-plume and 31 Ma trap basalts throughout Ethiopia and Yemen, and in northern Eritrea and parts of Yemen, this is marked by extensive laterites (Canuti et al. 1972; Zanettin et al. 1978; Davison et al. 1994; Sagri et al. 1998). Bohannon (1986) and Coleman (1993) considered this as evidence against significant pre-plume or pre-rift doming. However, pre-plume laterites are not known from central Afar itself, so the area of doming could have been fairly localized, or it may have been synchronous with the eruption of the earliest trap basalts (Burke 1996, reviewed in Şengör 2001).

The oldest syn-rift section in the southern Red Sea (offshore Eritrea) is marine and demonstrates a Late Oligocene seaway connection with the Gulf of Aden (Hughes et al. 1991; Hughes and Beydoun 1992). This paleogeographic detail limits how much Afar doming could have occurred along the focus of rifting. At the northern end of the Red Sea in the Gulf of Suez and vicinity of Cairo, stratigraphic relationships are similar though the rocks are somewhat younger: The Oligocene pre-rift strata are a mixture of shallow marine and low-relief fluvial facies, and with the exception of a few localized, very thin nonmarine beds, the syn-rift fill is essential all marine from the start of extension (Sellwood and Netherwood 1984; Richardson and Arthur 1988; Jackson 2008). The Cairo basalts are very consistent in thickness over a very large area, also suggesting a low-relief, flat pre-rift geometry (Bosworth et al. 2015). Garfunkel (1988) estimated that the maximum pre-rift erosion in western Sinai was a few hundred meters and that there was no evidence of uplift specific to the future rift axis.

Most geologic evidence favors superposition of Gulf of Aden and Red Sea rifting on a generally peneplaned surface that was near or in some areas below sea level. At the onset of extension, fault block rotation resulted in only very localized uplift, best documented in the Gulf of Suez (Garfunkel and Bartov 1977; Sellwood and Netherwood 1984; McClay et al. 1998; Carr et al. 2003). A total of 2–3 Myr after rift initiation, this situation changed dramatically. At about 20 Ma in the Gulf of Suez, depositional environments shifted from marginal to open marine with water depths of 200 m or more in sub-basin axes (Fig. 13d). Total compaction corrected subsidence rates increased by a factor of two or more (Steckler 1985; Moretti and Colletta 1987; Evans 1988; Richardson and Arthur 1988; Steckler et al. 1988). As discussed above, apatite fission track data indicate that this main phase of syn-rift subsidence was accompanied by unroofing and uplift of the rift shoulders along the entire length of the Red Sea rift system. These authors have proposed thermomechanical models linking the two processes.

The next major phase in the Red Sea continental rift history was marked by the onset of the Aqaba–Levant transform boundary (Fig. 13e). The arguments concerning the timing of this event are diverse (reviewed in Bosworth and McClay 2001; Bosworth et al. 2005) and generally suggest onset of left lateral shear in the Middle Miocene at ~14–12 Ma. Some authors have inferred a somewhat earlier initiation for the transform; for example, Garfunkel and Beyth (2006) proposed ~18–17 Ma in response to the beginning of oceanic spreading in the Gulf of Aden (discussed below). If the Gulf of Aqaba movement started in the Middle Miocene, then it corresponds to the time of collision of Arabia with Eurasia (Şengör and Yilmaz 1981; Hempton 1987; Woodruff and Savin 1989; Burke 1996). Offset of geologic features limits the total slip on this transform to be ~107 km of which 45 km is Pliocene to Recent (Quennell 1951, 1958). These data provide important kinematic constraints for Red Sea palinspastic restorations. With the onset of Aqaba–Levant motion, extension across the northern Red Sea changed from rift normal (NE–SW) to highly oblique and parallel to the transform (NNE–SSW, Fig. 13e).

Movement on the Aqaba–Levant transform is interpreted to have caused minor counterclockwise rotation of the new Sinai micro-plate and local compression and uplift in the northern Gulf of Suez (Fig. 13e; Patton et al. 1994). Middle Miocene sea level was also somewhat lowered (Haq et al. 1987), and the combined effect was that for the first time since the earliest Miocene the Gulf of Suez–Neotethyan seaway connection was largely severed. Open marine deposition was replaced by evaporitic conditions throughout most of the Gulf of Suez and northern Red Sea at ~12 Ma (intra-Serravallian; see stratigraphic discussion above). In the southern Red Sea, open marine shale was deposited offshore from Eritrea until the early part of the Late Miocene (Savoyat et al. 1989; Hughes and Beydoun 1992). The connection to the Gulf of Aden through Bab-al-Mandab therefore persisted somewhat longer, but by ~10 Ma (lower Tortonian), massive halite and anhydrite were being deposited throughout the Red Sea.

Oceanic Rifting

The easternmost and oldest segment of the oceanic spreading system of the Gulf of Aden–Red Sea rift is called the Sheba Ridge (Fig. 13d; Mathews et al. 1967). Spreading at the Sheba Ridge is thought to have started at ~19–18 Ma (Sahota 1990; Leroy et al. 2004), about 12 My after the

onset of continental rifting in this same area. Spreading was pinned at the Alula-Fartaq fracture zone for a few million years and then moved a few hundred kilometers west by ~16 Ma (Fig. 13e). By ~10 Ma, the spreading center had reached the Shukra el Sheik discontinuity in the western Gulf of Aden and was pinned again (Fig. 13f; Manighetti et al. 1997). Only after ~2 Ma did spreading propagate into Afar (Audin 1999; Hébert et al. 2001; Audin et al. 2004).

Oceanic spreading did not propagate from the western Gulf of Aden or Afar into the Red Sea. Rather, as discussed above based on magnetic striping, the oldest Red Sea spreading center appeared within the southern Red Sea continental rift at about 17°N latitude (Fig. 13g; Allan 1970; Röser 1975; Searle and Ross 1975). The age of initiation of spreading in this region was ~5 Ma (Cochran 1983). Since that time, complex volcanic activity and extensional faulting has continued within Afar west of the Danakil Alps (reviewed in Tefera et al. 1996; Redfield et al. 2003; Garfunkel and Beyth 2006). The Red Sea is linking to the Afar depression through the Gulf of Zulu and similarly to the Gulf of Aden through the Gulf of Tadjoura (Fig. 13h).

The length of the Gulf of Aden–Afar (subaerial)–Red Sea oceanic spreading center from the Carlsberg Ridge to the end of magnetic striping at about 19°N latitude in the southern Red Sea is ~2,800 km (Fig. 13h). As briefly outlined here and noted by many workers, the ridge propagated in pulses, but the average rate since inception at ~19 Ma is ~150 km/My. By comparison, the earlier continental rift system reaches from just east of Socotra Island–Ras Sharbithat (Fig. 13c; Stein and Cochran 1985) to NW of Cairo, a distance of ~3,900 km. The continental rift also developed in segments, and within each segment, age dating cannot resolve any discernible propagation. However, the entire rift was completed from 30 to 23 Ma or within 7 My. The average rate of advancement was ~550 km/My or nearly four times as rapid as growth of the later oceanic rift.

Discussion and Synthesis

The Red Sea offers great insight into how continental rifts form and subsequently can evolve into oceanic basins. But is this system a suitable model for many rift settings, or is it perhaps very unique or an end member type? As discussed at the introduction to this chapter, the Red Sea is both another phase in the long history of breakup of Gondwana, and the product of a tectonic environment shaped by impingement of large mantle plumes (particularly Afar) at the base of the African lithosphere. Adding complexity to this background is the ongoing collision of Africa–Arabia with Eurasia, and the modifications to plate boundaries produced by movement on the Aqaba–Levant transform margin.

Rift Driving Forces

Theoretical models and analyses of continental rifts often focus on two fundamental questions: (1) what are the driving forces for rifting? and (2) how do rifts grow (propagate) laterally? Milanovsky (1972) divided continental rifts into those associated with continental "platforms" and others found in young fold belts. The platform rifts were either typified by broad doming and abundant alkaline volcanism, or no doming and little or no volcanism. Sengör and Burke (1978) elaborated on these fundamental differences and proposed the terms "active" and "passive" rifting based on their interpretation of the underlying dynamics of these two rift types. In active rifts, extension is driven by upwelling mantle convection currents, while passive rifts are the result of far-field extensional stresses arising from lithospheric plate movement and plate boundary interactions. Utilizing finite element modeling, Dunbar and Sawyer (1988) proposed that both volcanic-rich domed rifts and non-volcanic crevice style rifts could be formed by regional extensional stresses without involvement of mantle currents. In their models, the surficial manifestations of rifting were controlled by the positions of weakness in the pre-rift lithosphere, whether in the crust or upper mantle. In a lithospheric plate subjected to extensional forces, uplift occurred above a mantle weakness, whereas fault-bounded basins formed above crustal weakness. Various combinations of these pre-existing weaknesses can be envisioned, and they might be laterally offset from each other or vertically superimposed. Buck (2006) however has argued that normal continental lithosphere may be too strong to rift without magmatic dike intrusion, and therefore, there must be an appropriate combination of regional extension and a source of sufficient magma. He suggested that both the Red Sea and Ethiopian Rift developed as magma-assisted rifts, whereas the model is difficult to apply to the Gulf of Aden where syn-rift dikes are absent.

Based on a synthesis of the timing of geologic events and the evolving geometry of the Arabian region, Bosworth et al. (2005) favored the interpretation that the principal driving forces for rifting in both the Gulf of Aden and Red Sea were far-field stresses, principally slab pull beneath the approaching Urumieh–Dokhtar arc (McQuarrie et al. 2003). Bosworth et al. considered the trigger for rifting to be the impingement of the Afar plume at ~31 Ma, and the actual onset of full-length Red Sea rifting the ~24–22 Ma dike event. The Bosworth et al. interpretation for the Red Sea is therefore compatible with Buck's theoretical considerations. The geometric association of the Gulf of Aden, Red Sea, and Ethiopian Rift with Afar—the classic Afar rift–rift–rift triple junction (Mohr 1970; McKenzie et al. 1970; Burke and Dewey 1973)—proves a role for the plume in rifting here.

It is critical, however, to recognize that during eruption of the Afar flood basalts, a triple junction did not exist (Fig. 13a) and that the various arms of the rift system evolved thereafter at discernibly different geologic times (Bosworth et al. 2005).

Reilinger and McClusky (2011) have synthesized geodetic (GPS) and plate tectonic observations for the Nubia–Arabia–Eurasia plate system and the Mediterranean basin. Their analysis further supports the interpretation that the primary driving force in this system derives from subduction of Neotethyan lithosphere beneath Eurasia (Jolivet and Faccenna 2000; McQuarrie et al. 2003; Faccenna et al. 2013). They correlate the initiation of extensional tectonics in the Mediterranean (Alboran, Belearic, and Aegean basins) with the ~50 % decrease in the rate of convergence between Africa and Eurasia at 24 ± 4 Ma, the onset of rifting in the Red Sea (they include continental rifting in the Gulf of Aden, which is incorrect as it is older; see discussion above). A second ~50 % decrease in convergence occurred when oceanic rifting developed along the entire Gulf of Aden and movement shifted from the Gulf of Suez to the Aqaba–Levant transform margin at 11 ± 2 Ma. This was also coeval with intensified extension in numerous Mediterranean basins.

Rift Propagation

Early models of "rift" propagation often really focused on how oceanic rifts (i.e., spreading centers/mid-ocean ridges) progress laterally through a precursor zone of continental extension (e.g., Vink 1982; Courtillot 1982; Martin 1984). Important questions included how much continental extension predates breakthrough of the oceanic rift, how the extension was physically accommodated (faulting versus igneous intrusion), the resulting diachronous nature of the continent–ocean boundary, and the relative roles of rigid plates and micro-plates (Burke and Whiteman 1973; Burke and Dewey 1974; Hey 1977; LePichon and Sibuet 1981). In the first step of these models, the onset of continental rifting is instantaneous across the ruptured plate. In later steps, the oceanic rift propagates over time through the extended lithosphere (generally toward a pole of rotation). An additional observation by Martin (1984) was that an oceanic spreading center could appear within a segment of stretched continental lithosphere without connection to a propagating ridge which is of relevance to the spreading center of the southern Red Sea.

Instantaneous rupture of the lithospheric plate is a requirement if plate tectonics is applied rigorously at all scales of observation. Alternatively if some degree of distributed deformation is allowed, then the rift zone can propagate by a process of "unzipping" (Omar and Steckler 1995). It is important to emphasize that Omar and Steckler were specifically discussing the onset of continental rifting; regardless of how this early separation occurred, the later development of an oceanic rift could proceed by a similar or different geometrical/kinematic history. Based on fission track data discussed above, Omar and Steckler concluded that continental rifting of the Red Sea occurred in two phases at ~34 Ma and 25–21 Ma and that in both instances the rifting was simultaneous along its entire length. No propagation could be discerned, and the tenets of rigid plate tectonics were upheld.

The end members of rift propagation models are illustrated in Fig. 14a, b. A minor modification of the propagating rift is the inclusion of a finite, approximately constant width rift valley that does the actual propagation. For the Red Sea and Gulf of Aden, Bosworth et al. (2005) suggested this would have been on the order of 60–80 km. Courtillot (1982) emphasized the importance of "locked zones" that impede the lateral growth of rifts. This process can occur in either continental or oceanic rift systems and is particularly well displayed in the oceanic rift history of the Gulf of Aden (Manighetti et al. 1997) as discussed above. Wijk and Blackman (2005) referred to this as a stalled rift mode. The stalling or locking of a rift would result in pulses of extension along a rift system (Fig. 14c). Between successive locked zones, the rift could either propagate laterally or instantaneously rupture the lithosphere (hybrid of either Fig. 14a or b). The locked zones could correspond to the positions of pre-rift lithospheric structures that might be favorably oriented to evolve into transform faults in the ultimate oceanic rift system. If unfavorably oriented, they might result in distributed deformation and not lead directly to a simple transform geometry (Fig. 14c).

Timing of rifting for the Gulf of Aden and Red Sea summarized above suggests that these basins experienced a stalled rift mode not only during oceanic rift propagation but also during the precursor continental rifting. By the Late Oligocene (~27.5 Ma), extension and syn-rift sedimentation were occurring throughout the Gulf of Aden and into the southernmost Red Sea offshore present-day Eritrea. Rifting did not move north, based on presently available data, until about 3.5 My later. When the next rift segment developed, it jumped immediately to northern Egypt based on the age of the associated dike event (Table 1), as proposed by Omar and Steckler (1995). Lyakhovsky et al. (2012) have emphasized that an important parameter during rift propagation is the long-term memory effect of fractured rocks. It is possible that during the 3.5 My stall, the pre-Red Sea lithosphere was being pre-conditioned/weakened for rifting by a period of focused brittle deformation without significant surface extension.

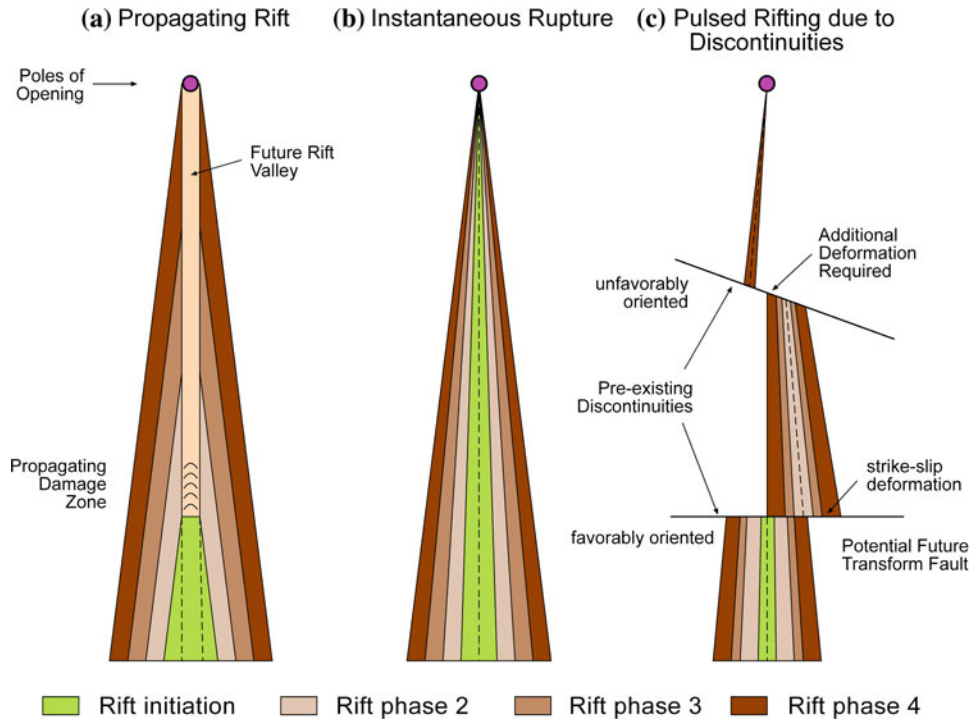

Fig. 14 Modes of continental rift propagation. **a** and **b** are traditional models of propagating (unzipping) and instantaneously rupturing rifts; **c** is a pulsed rift history in which the basin undergoes phases of stalling or locking at pre-existing discontinuities. After passing a locked zone, the rift can switch to the style of either (**a**) or (**b**). The stalled mode is common in oceanic rifts (Courtillot 1982; Van Wijk and Blackman 2005). The colors are meant to show the overall width of the rift growing through time (stretching of the lithosphere) and not age of accreted material which would be the case in oceanic rifts. The Gulf of Aden–Red Sea rift system developed as in (**c**), with individual segments rupturing instantaneously as far as geologic data can presently discern

Northern and Southern Red Sea Comparison

A plausible Red Sea regional model can be summarized as follows: (1) The early phase of purely continental rifting is represented by the Gulf of Suez; (2) a continental rift that is beginning to show some expression of oceanic rifting is seen in the northern Red Sea; and (3) a young oceanic basin that has entered the early phase of drift is found in the southern Red Sea (see discussions in Cochran 1983, 2005; Bonatti 1985; Martinez and Cochran 1988; Girdler 1991; Coleman 1993). In line with this often accepted progression of rifting styles, Cochran (2005) interpreted the presence of large, rotated fault blocks in the northern Red Sea with faults that sole into a zone of plastic creep in the lower crust. This keeps the Moho flat but allows the observed high upper crustal relief. Through time extension is focused at the rift axis, the lithosphere thins rapidly and melt is generated. One product of this is the small axial volcanoes present in some of the axial deeps, which with further extension and magmatism would coalesce into cells of seafloor spreading.

It is now recognized that some of the Earth's magma-poor continental margins did not develop an oceanic spreading center until they were truly hyperextended with continental mantle rocks exposed at the seafloor (Whitmarsh et al. 2001; Henning et al. 2004; Sutra and Manatschal 2012 and references therein). Developed originally with data and interpretations from the west Iberia margin and Alpine Tethyan exposures, the models proposed for these margins invoke development of a wide zone of upper crustal rift basins and rotated fault blocks above ductile, distributed deformation in a weak lower or middle crust. Deformation history and geometry are complex and varied, but a common theme is that eventually concave downward exhumation faults bring subcontinental mantle rocks to the seafloor. An oceanic spreading center is delayed until later and ultimately forms in a position controlled by weaknesses in the subcontinental lithospheric mantle and the thermal structure of the rising asthenospheric mantle. The juncture between the hyperextended crust (≤10 km) and normal crust (~30 km) is commonly abrupt and is referred to as the "necking zone" (Mohn et al. 2012). The northern Red Sea at the Brothers Islands is ~190 km wide today (Fig. 2b). In a pre-rift configuration, this area was ~45 km wide (Fig. 6). Ignoring the role of the low-strain onshore fault blocks and assuming

purely mechanical extension, this gives a β factor of greater than four—this is certainly a candidate for a hyperextended terrane. As discussed above, geophysical data suggest that there is also a necking zone along both coastlines though most pronounced on the Egyptian margin (Voggenreiter et al. 1988).

Much less is known about the structure of the southern Red Sea, though there is no question that the amount of opening is considerably greater than in the north (Le Pichon and Francheteau 1978; Joffe and Garfunkel 1987). A free-air gravity anomaly map derived from satellite altimetry (Smith and Sandwell 1997) presented by Cochran and Karner (2007) lacks evidence of prominent linear rift-parallel gravity highs and lows like those of the north, and this is interpreted to reflect a lack of large, rotated fault blocks. Cochran and Karner (2007) suggested that the southern Red Sea resembles the West African and Brazilian passive continental margins in this respect, where regional syn-rift sag basins dominate (Karner et al. 2003). They proposed that proximity to the Afar plume weakened the lithosphere beneath the southern Red Sea (Burke 1996; Courtillot et al. 1999) and that this is resulting in widely differing responses to extension in the north and south.

In addition to the effects of distance from the Afar plume, other authors have described the role that the Aqaba–Levant transform boundary (Dead Sea fault) has played in differentiating the behavior of the northern Red Sea from that of the south (Ben Avraham 1985, 1987; Ben-Avraham and Von Herzen 1987; Ben-Avraham et al. 2008; Lazar et al. 2012). It seems very plausible that the presence of this plate boundary should have a significant impact on mantle convection beneath the northern Red Sea and perhaps the mode of crustal deformation.

Figure 13c shows a compilation of where continental extension was occurring at ~24 Ma, when the main Red Sea dike event took place and deformation reached the margin of Neotethys in the north. In the southern and central Red Sea, crustal effects of rifting (faulting, volcanism) never exceeded about 200 km in width. In the north, however, deformation was distributed over a much broader area, from the Western Desert of Egypt to the Azraq–Sirhan graben in Jordan and Israel or on the order of 1,000 km (Segev and Rybakov 2011; Lyakhovsky et al. 2012; Szymanski 2013; Bosworth et al. 2015). Significant Red Sea extension or volcanism is not observed north of the Egyptian Mediterranean coastline. If the Mediterranean basin overlies oceanic lithosphere, it would generally be too strong to rupture (e.g., Vink et al. 1984). Steckler and ten Brink (1986) suggested that this is why the Red Sea plate boundary subsequently shifted to the Aqaba–Levant transform and abandoned the Gulf of Suez (see further discussion in Lyakhovsky et al. 2012). The very broad zone of early northern Red Sea extension might reflect initial interaction of the Red Sea rift with this impenetrable oceanic barrier.

Two Plume Model

The 24–22 Ma basaltic volcanism of northern Egypt is not sufficiently voluminous to be considered the product of a mantle plume in a traditional sense. However, the minimum preserved subsurface area of 15,000 km^2 and an average thickness of ~30 m (Fig. 11) give an erupted volume of 450 km^3 to which should be added the smaller flows of the northern Gulf of Suez and Bahariya Oasis. As discussed above, trace element and Sr–Nd–Pb–Hf isotope analyses suggest that these sub-alkaline basalts were derived from mixing of an Afar plume-like source with metasomatized spinel-facies continental lithosphere (Endress et al. 2011). Endress et al. relate this and other North African mid-Cenozoic magmatic activity to upwelling mantle material from the northern margins of the South African Superplume. Bosworth et al. (2015) refer the northern Egypt volcanism to the effects of a Cairo "mini-plume" (Fig. 15).

Field and subsurface observations indicate that the Cairo and Gulf of Suez volcanism were coeval with the onset of NE–SW extension and the deposition of syn-rift sediments (see

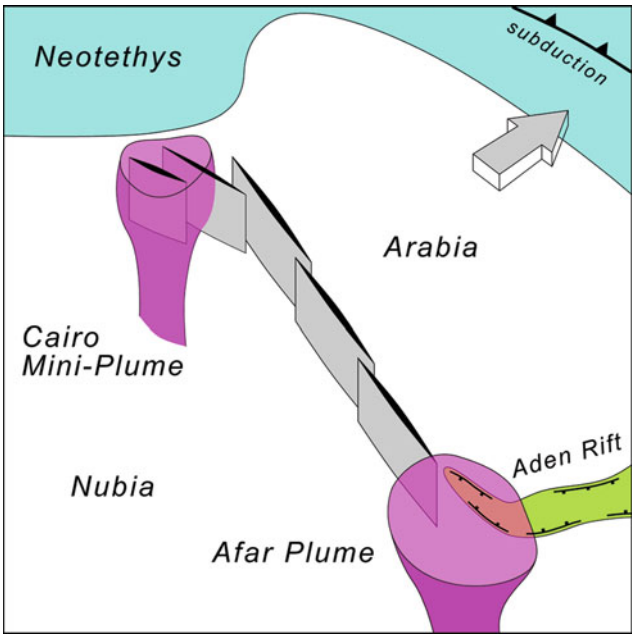

Fig. 15 Two-plume model for the origin of the Red Sea continental rift. Basaltic dikes (shown in *gray*) that link the Afar plume to the Cairo mini-plume at 24–22 Ma are drawn schematically. At the surface, they are much smaller, narrower, and numerous; their geometry at depth is unknown. The feathering into a broader zone of intrusion in the north however is real

above). For most of the area of the Cairo basalts, the amount of extension is very small, and structuring did not significantly impact the distribution of the main flows. But initial rift faults did occupy the area of just east of Bahariya to the east side of the Gulf of Suez, with the basaltic volcanism focused at the middle of this broad zone. Only minor basaltic dikes and flows are actually associated with the ultimate focus of extension along the Gulf of Suez and Northern Red Sea. For these reasons, it seems that rifting did not generate the basalts, but rather the basalts may have helped control the direction of the rift as it shot north from Eritrea, perhaps in conjunction with a stress concentration at the bend in the Levant–Mediterranean continental margin (Burke 1996). The Cairo mini-plume may have acted as a trigger for the last phase of Red Sea rift propagation, similar to the role proposed for the Afar plume for Gulf of Aden continental rifting (Bosworth et al. 2005).

Summary

The Red Sea is part of an extensive rift system that includes from south to north the oceanic Sheba Ridge, the Gulf of Aden, the Afar region, the Red Sea, the Gulf of Aqaba, the Gulf of Suez, and the Cairo basalt province. Historical interest in this area has stemmed from many causes with diverse objectives, but it is best known as a potential model for how continental lithosphere first ruptures and then evolves to oceanic spreading, a key segment of the Wilson cycle and plate tectonics. Abundant and complementary datasets, from outcrop geology, geochronologic studies, refraction and reflection seismic surveys, gravity and magnetic surveys, to geodesy, have facilitated these studies. Magnetically striped oceanic crust is present in the Gulf of Aden and southern Red Sea, active magma systems are observed onshore in the Afar, highly extended continental or mixed crust submerged beneath several kilometers of seawater is present in the northern Red Sea, and a continental rift is undergoing uplift and exposure in the Gulf of Suez. The greater Red Sea rift system therefore provides insights into all phases of rift-to-drift histories.

Many questions remain about the subsurface structure of the Red Sea and the forces that led to its creation. However, the timing of events, both in an absolute sense and relative to each other, is becoming increasingly well constrained. Six main steps may be recognized: (1) Plume-related basaltic trap volcanism began in Ethiopia, NE Sudan (Derudeb), and SW Yemen at ~31 Ma, followed by rhyolitic volcanism at ~30 Ma. Volcanism thereafter spread northward to Harrats Sirat, Hadan, Ishara-Khirsat, and Ar Rahat in western Saudi Arabia. This early magmatism occurred without significant extension or at least none that has yet been demonstrated. It is often suggested that this "Afar" plume triggered the onset of Aden–Red Sea rifting, or in some models, it was the main driving force. (2) Starting between ~29.9 and 28.7 Ma, marine syn-tectonic sediments were deposited on continental crust in the central Gulf of Aden. Therefore, Early Oligocene rifting is established to the east of Afar. Whether rifting propagated from the vicinity of the Sheba Ridge toward Afar, or the opposite, or essentially appeared synchronously throughout the Gulf of Aden is not yet known. 3) By ~27.5–23.8 Ma, a small rift basin was forming in the Eritrean Red Sea. At approximately the same time (~25 Ma), extension and rifting commenced within Afar itself. The birth of the Red Sea as a rift basin is therefore a Late Oligocene event. (4) At ~24–23 Ma, a new phase of volcanism, principally basaltic dikes but also layered gabbro and granophyre bodies, appeared nearly synchronously throughout the entire Red Sea, from Afar and Yemen to northern Egypt. The result was that the Red Sea rift briefly linked two very active volcanic centers covering 15,000–25,000 km^2 in the north and >600,000 km^2 in the south. The presence of the "mini-plume" in northern Egypt may have played a role somewhat analogous to Afar vis-à-vis the triggering of the dike event. The 24–23 Ma magmatism was accompanied by strong rift-normal extension and deposition of syn-tectonic sediments, mostly of marine and marginal marine affinity. The area of extension in the north was very broad, on the order of 1,000 km, and much narrower in the south, about 200 km or less. Throughout the Red Sea, the principal phase of rift shoulder uplift and rapid syn-rift subsidence followed shortly thereafter. Synchronous with the appearance of extension throughout the entire Red Sea, relative convergence between Africa and Eurasia slowed by about 50 %. (5) At ~14–12 Ma, a transform boundary cut through Sinai and the Levant continental margin, linking the northern Red Sea with the Bitlis–Zagros convergence zone. This corresponded with collision of Arabia and Eurasia, which resulted in a new plate geometry with different boundary forces. Red Sea extension changed from rift normal (N60°E) to highly oblique and parallel to the Aqaba–Levant transform (N15°E). Extension across the Gulf of Suez decreased by about a factor of 10, and convergence between Africa and Eurasia again dropped by about 50 %. In the Afar region, Red Sea extension shifted from offshore Eritrea to west of the Danakil horst, and activity began in the northern Ethiopian rift. (6) These early events or phases all took place within continental lithosphere and formed a continental rift system 4,000 km in length. When the lithosphere was sufficiently thinned, an organized oceanic spreading center was established and the rift-to-drift transition started. Oceanic spreading initiated first on the Sheba Ridge east of the Alula-Fartaq fracture zone at ~19–18 Ma. After stalling at this fracture zone, the ridge probably propagated west into the central Gulf of Aden by ~16 Ma. This matches the observed termination of syn-tectonic deposition along the onshore Aden margins at approximately

the same time. At ~10 Ma, the Sheba Ridge rapidly propagated west over 400 km from the central Gulf of Aden to the Shukra al Sheik discontinuity. Oceanic spreading followed in the south-central Red Sea at ~5 Ma. This spreading center was initially not connected to the spreading center of the Gulf of Aden. By ~3–2 Ma, oceanic spreading moved west of the Shukra al Sheik discontinuity, and the entire Gulf of Aden was an oceanic rift. During the last ~1 My, the southern Red Sea plate boundary linked to the Aden spreading center through the Gulf of Zula, Danakil Depression, and Gulf of Tadjoura.

Presently, the Red Sea spreading center may be propagating toward the northern Red Sea to link with the Aqaba–Levant transform. However, important differences appear to exist between the southern and northern Red Sea basins, both in terms of the nature of the pre- to syn-rift lithospheric properties and the response to plate separation. If as favored here no oceanic spreading is present in the northern Red Sea, then it is a magma-poor hyperextended basin with β factor >4 that is evolving in many ways like the west Iberia margin. Testing, this hypothesis will require the acquisition of deep reflection seismic profiles from margin to margin and the drilling of more offshore wells (Steckler et al. 2001). It is probable that the ultimate geometries of the northern and southern Red Sea passive margins will be very different. The Red Sea provides an outstanding area in which to study the rift-to-drift transition of continental disruption, but it is unlikely to be a precise analogue for all passive continental margin histories.

Acknowledgments Philippe Huchon and Ken McClay collaborated with me on an earlier synthesis of the Red Sea and Gulf of Aden, and their past research and interpretations have heavily influenced what is presented in this chapter. Daniel Stockli, Daniel Helgeson, and Michael Cosca are co-researchers on the Cairo plume and circa 23 Ma dike event, and their efforts and perseverance are very much appreciated. James Cochran very kindly provided me with his digital compilation of northern Red Sea bathymetric data. I have had the great pleasure to work with many scientists in the field in the Gulf of Suez and Red Sea and I thank them all. Nickolas Raterman and William Wescott kindly reviewed the manuscript and suggested many important improvements. Stockli and Raterman impressed upon me the similarities of magma-poor hyperextended margins and the northern Red Sea. Kevin Burke has been my patient mentor regarding all things rifting, plumes, and the Red Sea in particular. I sincerely thank him for this.

References

Abbate E, Balestrieri ML, Bigazzi G (2002) Morphostructural development of the Eritrean rift flank (southern Red Sea) inferred from apatite fission track analysis. J Geophys Res 107(B11):11

Ali Kassim M, Carmignani L, Conti P, Fantozzi PL (2002) Geology of the Mesozoic-Tertiary sedimentary basins in southwestern Somalia. J Afr Earth Sci 34:3–20

Allan TD (1970) Magnetic and gravity fields over the Red Sea. Philos Trans R Soc Lond 267:153–180

Allan TD, Charnock H, Morelli C (1964) Magnetic, gravity and depth surveys in the Mediterranean and Red Sea. Nature 204:1245–1248

Alsharhan AS (2003) Petroleum geology and potential hydrocarbon plays in the Gulf of Suez rift basin, Egypt. Am Assoc Pet Geol Bull 87:143–180

Ameen MS (2014) Fracture and in-situ stress patterns and impact on performance in the Khuff structural prospects, eastern offshore Saudi Arabia. Mar Pet Geol 50:166–184

Anderson DL (1982) Hotspots, polar wander, Mesozoic convection, and the geoid. Nature 297:391–393

Angelier J (1985) Extension and rifting: the Zeit region, Gulf of Suez. J Struct Geol 7:605–612

Argand E (1924) La Tectonique de l'Asie. In: Proceedings of the 13th international geological congress, vol 1, pp 171–372

ArRajehi A, McClusky S, Reilinger R, Daoud M, Alchalbi A, Ergintav S, Gomez F, Sholan J, Bou-Rabee F, Ogubazghi G, Haileab B, Fisseha S, Asfaw L, Mahmoud S, Rayan A, Bendik R, Kogan L (2010) Geodetic constraints on present-day motion of the Arabian Plate: implications for Red Sea and Gulf of Aden rifting. Tectonics 29

Audin L (1999) Pénétration de la dorsale d'Aden dans la depression Afar entre 20 et 4 Ma. PhD thesis, Université de Paris 7 et Institut de Physique du Globe de Paris, Paris, 278 pp

Audin L, Quidelleur X, Coulié E, Courtillot V, Gilder S, Manighetti I, Gillot P-Y, Tapponnier P, Kidane T (2004) Paleomagnetism and K-Ar and 40Ar/39Ar ages in the Ali Sabieh area (Republic of Djibouti and Ethiopia): constraints on the mechanism of Aden ridge propagation into southeastern Afar during the last 10 Myr. Geophys J Int 158:327–345

Bailey DK (1992) Episodic alkaline igneous activity across Africa; implications for the causes of continental break-up. Geol Soc London Spec Publ 68:91–98

Bailey DK (1993) Carbonate magmas. J Geol Soc London 150:637–651

Baker BH (1970) The structural pattern of the Afro-Arabian rift system in relation to plate tectonics. Philos Trans Royal Soc London Series A Math Phys Sci 267:383–391

Baker J, Menzies M, Snee L (1994) Stratigraphy, $^{40}Ar/^{39}Ar$ geochronology and geochemistry of flood volcanism in Yemen. Mineral Mag 58A:42–43

Baker J, Snee L, Menzies M (1996) A brief Oligocene period of flood volcanism in Yemen: implications for the duration and rate of continental flood volcanism at the Afro-Arabian triple junction. Earth Planet Sci Lett 138:39–55

Barakat H, Miller P (1984) Geology and petroleum exploration, Safaga Concession, northern Red Sea, Egypt. In: Proceedings of the 7th exploration seminar, Egyptian General Petroleum Corporation, Cairo, pp 191–214

Barberi F, Giglia G, Marinelli G, Santacroce R, Tazieff H, Varet J (1971) Carte geologique du Nord de l'Afar, scale 1:500,000. CNR-CNRS, La Celle-St Cloud

Barberi F, Borsi S, Ferrara G, Marinelli G, Santacroce R, Tazieff H, Varet J (1972) Evolution of the Danakil Depression (Afar, Ethiopia) in light of radiometric age determinations. J Geol 80:720–729

Barberi F, Santacroce R, Varet J (1975) Structural evolution of the Afar triple junction. In: Pilger A, Rösler A (eds) Afar depression of Ethiopia, Proceedings of an international symposium on the afar region and related rift problems, vol 1. Bad Bergzabern FR, Germany, 1–6 April 1974. E. Schweizerbartsche Verlagsbuchhandlung, Stuttgart, pp 38–54

Basile C, Mascle J, Guiraud R (2005) Phanerozoic geological evolution of the equatorial atlantic domain. In: Catuneanu O, Guiraud R, Eriksson P, Thomas B, Shone R, Key R (eds) Phanerozoic evolution of Africa. J Afr Earth Sci 43:275–282

Ben-Avraham Z (1985) Structural framework of the Gulf of Elat (Aqaba)—northern Red Sea. J Geophys Res 90:703–726

Ben-Avraham Z (1987) Rift propagation along the southern Dead Sea rift (Gulf of Elat). Tectonophysics 143:193–200

Ben-Avraham Z, Von Herzen RP (1987) Heat flow and continental breakup: the Gulf of Elat (Aqaba). J Geophys Res 92:1407–1416
Ben-Avraham Z, Garfunkel Z, Lazar M (2008) Geology and evolution of the southern Dead Sea fault with emphasis on subsurface structure. Annu Rev Earth Planet Sci 36:357–387
Bender F (1975) Geology of the arabian peninsula, Jordan. U.S. Geological Survey Professional Paper 560-D
Berhe SM (1986) Geologic and geochronologic constraints on the evolution of the Red Sea-Gulf of Aden and Afar depression. J Afr Earth Sci 5:101–117
Beydoun ZR (1978) Southern Arabia and northern Somalia: comparative geology. Philosophical Transactions of the Royal Society (London) Series A, pp 267–292
Beydoun ZR (1989) Hydrocarbon prospects of the Red Sea-Gulf of Aden; a review. J Pet Geol 12:125–144
Beydoun ZR, Sikander AH (1992) The Red Sea-Gulf of Aden: reassessment of hydrocarbon potential. Mar Pet Geol 9:474–485
Bicknell JD, MacDonald KC, Miller SP, Lonsdale PF, Becker K (1986) Tectonics of the Nereus Deep, Red Sea: a deep tow investigation of a site of initial rifting. Mar Geophys Res 8:131–148
Blank HR, Mooney WD, Healy JH, Gettings MA, Lamson RJ (1986) A seismic refraction interpretation of the eastern margin of the Red Sea depression, Southwest Saudi Arabia. U.S. Geological Survey Open-File Report 86–257, 20 pp
Blow WH (1969) Late middle Eocene to recent planktonic foraminiferal biostratigraphy. In: Bronniman R (ed) Proceedings of the 1st international conference on planktonic microfossils, vol 1. Geneva, 1967, Brill, Leiden, pp 199–421
Bohannon RG (1986) Tectonic configuration of the western Arabian continental margin, southern Red Sea. Tectonics 5:477–499
Bohannon RG, Naeser CW, Schmidt DL, Zimmerman RA (1989) The timing of uplift, volcanism, and rifting peripheral to the Red Sea: a case for passive rifting? J Geophys Res 94:1683–1701
Bonatti E (1985) Punctiform initiation of seafloor spreading in the Red Sea during transition from a continental to an oceanic rift. Nature 316:33–37
Bonatti E, Colantoni P, Della Vedova B, Taviani M (1984) Geology of the Red Sea transitional zone (22°N–25°N). Oceanol Acta 7:385–398
Bosence DWJ, Al-Awah MH, Davison I, Rosen BR, Vita-Finzi C, Whittaker E (1998) Salt domes and their control on basin margin sedimentation: a case study from the Tihama plain, Yemen. In: Purser BH, Bosence DWJ (eds) Sedimentation and tectonics in Rift Basins—Red Sea—Gulf of Aden. Chapman and Hall, London, pp 448–466
Bosworth W (1985) Geometry of propagating continental rifts. Nature 316:625–627
Bosworth W (1992) Mesozoic and early Tertiary rift tectonics in East Africa. Tectonophysics 209:115–137
Bosworth W (1993) Nature of the Red Sea crust: a controversy revisited: comment. Geology 21:574–575
Bosworth W (1994) A model for the three-dimensional evolution of continental rift basins, north-east Africa. Geol Rundsch 83:671–688
Bosworth W (1995) A high-strain rift model for the southern Gulf of Suez (Egypt). In: Lambiase JJ (ed) Hydrocarbon habitat in Rift basins. Geological Society, London, Special Paper 80, pp 75–102
Bosworth W, Burke K (2005) Evolution of the Red Sea—Gulf of Aden rift system. In: Post PJ, Rosen NC, Olson DL, Palmes SL, Lyons KT, Newton GB (eds) Petroleum systems of divergent continental margin basins. 2005 Gulf Coast Section SEPM Foundation 25th Bob F. Perkins Annual Research Conference, Houston, 4–7 Dec, 2005, CD-ROM, pp 342–372
Bosworth W, McClay K (2001) Structural and stratigraphic evolution of the Gulf of Suez rift, Egypt: A synthesis. In: Ziegler PA, Cavazza W, Robertson AHF, Crasquin-Soleau S (eds) Peri-Tethys Memoir 6: Peri-Tethyan Rift/Wrench basins and passive margins, vol 186. Mémoires du Muséum National d'Histoire Naturelle de Paris, pp 567–606
Bosworth W, Strecker MR (1997) Stress field changes in the Afro-Arabian rift system during the Miocene to recent period. Tectonophyscis 278:47–62
Bosworth W, Crevello P, Winn RD Jr, Steinmetz J (1998) Structure, sedimentation, and basin dynamics during rifting of the Gulf of Suez and northwestern Red Sea. In: Purser BH, Bosence DWJ (eds) Sedimentation and Tectonics of Rift basins: Red Sea-Gulf of Aden. Chapman and Hall, London, pp 77–96
Bosworth W, Darwish M, Crevello P, Taviani M, Marshak S (1996) Stratigraphic and structural evolution of Zabargad Island (Red Sea, Egypt) since the Early Cretaceous. In: Youssef El SA (ed) Proceedings of the 3rd international conference on geology of the Arab World, vol 1, pp 161–190
Bosworth W, Huchon P, McClay K(2005) The Red Sea and Gulf of Aden Basins. In: Catuneanu O, Guiraud R, EriksonP, Thomas B, Shone R, Key R(eds) Phanerozoic evolution of Africa. J Afr Earth Sci 43:334–378
Bosworth W, Khalil S, Clare A, Comisky J, Abdelal H, Reed T, Kokkoros G (2012) Integration of outcrop and subsurface data during the development of a naturally fractured Eocene carbonate reservoir at the East Ras Budran concession, Gulf of Suez, Egypt. In: Spence GH, Redfern J, Aguilera R, Bevan TG, Cosgrove JW, Couples GD, Daniel J-M (eds) Advances in the study of fractured reservoirs, vol 374. Geological Society, London, Special Publications, 27 pp
Bosworth W, Stockli DF, Helgeson DE, Cosca M (2015) Integrated outcrop, 3D seismic, and geochronologic interpretation of Red Sea dike-related deformation (ca. 23 Ma) in the Western Desert, Egypt—the role of the Cairo "mini-plume" (in press)
Bott WF, Smith BA, Oakes G, Sikander AH, Ibrahim AI (1992) The tectonic framework and regional hydrocarbon prospectivity of the Gulf of Aden. J Pet Geol 15:211–243
Brinckmann J, Kursten M (1969) Geological sketchmap of the Danakil depression, 1: 250,000 scale. Bundesanstaldt für Bodenforschung, Hanover
Brown GF (1972) Tectonic map of the Arabian Peninsula: Map AP-2, scale 1: 4,000,000. Saudi Arabian Directorate General of Mineral Resources, Jeddah
Brown GF, Schmidt DL, Huffman ACJ (1989) Geology of the Arabian Peninsula, shield area of western Saudi Arabia. U.S. Geological Survey Professional Paper 560-A, 188 pp
Buck WR (2006) The role of magma in the development of the Afro-Arabian rift system. In: Yirgu G, Ebinger CJ, Maguire PKH (eds) The Afar volcanic province within the East African Rift System. Geological Society Special Publication, London, vol 259, pp 43–54
Buck WR, Martinez F, Steckler MS, Cochran JR (1988) Thermal consequences of lithospheric extension: pure and simple. Tectonics 7:213–234
Bumby AJ, Guiraud R (2005) The geodynamic setting of the Phanerozoic basins of Africa. J Afr Earth Sc 43:1–12
Bunter MAG, Abdel Magid AEM (1989) The Sudanese Red Sea; 1, New developments in stratigraphy and petroleum-geological evolution. J Pet Geol 12:145–166
Burke K (1996) The African plate. S Afr J Geol 99:341–409
Burke K, Dewey JF (1973) Plume-generated triple junctions: key indicators in applying plate tectonics to old rocks. J Geol 81:406–433
Burke K, Dewey JF (1974) Two plates in Africa in the cretaceous? Nature 249:313–316
Burke K, Gunnell Y (2008) The African erosion surface; a continental-scale synthesis of geomorphology, tectonics, and environmental change over the past 180 million years. Geological Society of America Memoir, vol 201, 66 pp
Burke K, Whiteman AJ (1973) Uplift, rifting and the break-up of Africa. In: Tarling DH (ed) Proceedings of the NATO conference on continental drift, Newcastle, vol 2. Academic Press, London, pp 735–745

Burke K, Wilson JT (1972) Is the African plate stationary? Nature 239:387–390

Canuti P, Gregnanin A, Piccirillo EM, Sagri M, Tacconi P (1972) Volcanic intercalation in the Mesozoic sediments of the Kulubi area (Harrar, Ethiopia). Bollettino della Societa Geologica Italiana 91:603–614

Carr ID, Gawthorpe RL, Jackson CAL, Sharp IR, Sadek A (2003) Sedimentology and sequence stratigraphy of early syn-rift tidal sediments: the Nukhul Formation, Suez Rift. Egypt. J Sediment Res 73:407–420

Chernet T, Hart WK, Aronson JL, Walter RC (1998) New age constraints on the timing of volcanism and tectonism in the northern Main Ethiopian Rift-southern Afar transition zone (Ethiopia). J Volcanol Geoth Res 80:267–280

Clin M, Pouchan P (1970) Carte Geologique du Territore Française des Afars et des Issas, 1:200,000 scale. Centre d'Etudes Geologique et de Development du T.F.A.I, Djibouti

Cochran JR (1983) A model for development of the Red Sea. Bull Am Assoc Petrol Geol 67:41–69

Cochran JR (2005) Northern Red Sea: nucleation of an oceanic spreading center within a continental rift. Geochem Geophys Geosyst 6:Q03006

Cochran JR, Karner GD (2007) Constraints on the deformation and rupturing of continental lithosphere of the Red Sea: the transition from rifting to drifting. In: Karner GD, Manatschal G, Pinheiro LM (eds) Imaging, mapping and modelling continental lithosphere extension and breakup, vol 282. Geological Society, London, Special Publications, pp 265–289

Cochran JR, Martinez F, Steckler MS, Hobart MA (1986) Conrad Deep: a new northern Red Sea deep: origin and implications for continental rifting. Earth Planet Sci Lett 78:18–32

Cochran JR, Martinez F (1988) Evidence from the northern Red Sea on the transition from continental to oceanic rifting. Tectonophysics 153:25–53

Coleman RG (1974) Geologic background of the Red Sea. In: Whitmarsh RB, Weser OE, Ross DA et al (eds) Initial reports of the deep sea drilling project, vol 23. Government Printing Office, Washington, pp 813–819

Coleman RG (1993) Geologic evolution of the Red Sea. Oxford monographs on geology and geophysics, vol 24. Oxford University Press, Oxford,186 pp

Coleman RG, Gregory RT, Brown GF (1983) Cenozoic volcanic rocks of Saudi Arabia. USGS Open-File Report 83-788, 82 pp

Colletta B, Le Quellec P, Letouzey J, Moretti I (1988) Longitudinal evolution of the Suez rift structure (Egypt). Tectonophysics 153:221–233

Collins WJ (2003) Slab pull, mantle convection, and Pangaean assembly and dispersal. Earth Planet Sci Lett 205:225–237

Coulié E, Quidelleur X, Gillot P-Y, Courtillot V, Lefèvre J-C, Chiesa S (2003) Comparative K-Ar and Ar/Ar dating of Ethiopian and Yemenite Oligocene volcanism: implications for timing and duration of the Ethiopian traps. Earth Planet Sci Lett 206:477–492

Courtillot V (1982) Propagating rifts and continental breakup. Tectonics 1:239–250

Courtillot V, Armijo R, Tapponnier P (1987) Kinematics of the Sinai triple junction and a two phase model of Arabia-Africa rifting. In: Coward MP, Dewey JF, Hancock PL (eds) Continental extensional tectonics, vol 28. Geological Society, London, Special Publication, pp 559–573

Courtillot V, Jaupart C, Manighetti I, Tapponnier P, Besse J (1999) On causal links between flood basalts and continental breakup. Earth Planet Sci Lett 166:177–195

Cross NE, Purser BH, Bosence DWJ (1998) The tectono-sedimentary evolution of a rift margin carbonate platform: Abu Shaar, Gulf of Suez, Egypt. In: Purser BH, Bosence DWJ (eds) Sedimentation and tectonics of rift basins: Red Sea-Gulf of Aden. Chapman and Hall, London, pp 271–295

Davies GF, Richards MA (1992) Mantle convection. J Geol 100:151–206

Davison I (2005) Central Atlantic margin basins of North West Africa: Geology and hydrocarbon potential (Morocco to Guinea). J Afr Earth Sci 43:254–274

Davison I, Al-Kadasi M, Al-Khirbash S, Al-Subbary AK, Baker J, Blakey S, Bosence D, Dart C, Heaton R, McClay K, Menzies M, Nichols G, Owen L, Yelland A (1994) Geological evolution of the southeastern Red Sea Rift margin, Republic of Yemen. Geol Soc Am Bull 106:1474–1493

Degens ET, Ross DA (eds) (1969) Hot brines and recent heavy metal deposits in the Red Sea a geochemical and geophysical account. Springer, New York, 571 pp

Drake CL, Girdler RW (1964) A geophysical study of the Red Sea. Geophys J Roy Astron Soc 8:473–495

Dunbar JA, Sawyer DS (1988) Continental rifting at pre-existing lithospheric weaknesses. Nature 333:450–452

Egyptian General Petroleum Corporation (1996) Gulf of Suez Oil Fields (a comprehensive overview). The Egyptian General Petroleum Corporation, New Maadi, 736 pp

El Atfy H, Brocke R, Uhl D (2013) A fungal proliferation near the probably Oligocene/Miocene boundary, Nukhul Formation, Gulf of Suez, Egypt. J Micropalaeontology 32:183–195

El-Shafy AA (1992) Miocene-Pliocene boundary in the Gulf of Suez-Region, Egypt. In: Proceedings of the 10th petroleum exploration and production conference vol 1. Cairo, November, 1990, Egyptian General Petroleum Corporation, Cairo, pp 213–232

Endress C, Furman T, Abu El-Rus MA, Hanan BB (2011) Geochemistry of 24 Ma basalts from NE Egypt: source components and fractionation history. In Van Hinsbergen DJJ, Buiter SJH, Torsvik TH, Gaina C, Webb SJ (eds) The formation and evolution of Africa: a synopsis of 3.8 Ga of Earth history vol 357. Geological Society Special Publications, London, pp 265–283

Evans AL (1988) Neogene tectonic and stratigraphic events in the Gulf of Suez rift area, Egypt. Tectonophysics 153:235–247

Eyal M, Bartov Y, Shimron AE, Bentor YK (1980) Geological map of the Sinai, scale 1:500,000. Geological Survey of Israel, Jerusalem

Faccenna C, Becker TW, Jolivet L, Keskin M (2013) Mantle convection in the Middle East: reconciling afar upwelling, Arabia indentation and Aegean trench rollback. Earth Planet Sci Lett 375:254–269

Fairhead JD (1988) Mesozoic plate tectonic reconstructions of the central South Atlantic Ocean: the role of the West and Central African rift system. Tectonophysics 155:181–191

Fantozzi PL, Sgavetti M (1998) Tectonic and sedimentary evolution of the eastern Gulf of Aden continental margins: new structural and stratigraphic data from Somalia and Yemen. In: Purser BH, Bosence DWJ (eds) Sedimentation and tectonics of Rift Basins: Red Sea—Gulf of Aden. Chapman and Hall, London, pp 56–76

Féraud G, Zumbo V, Sebai A, Bertrand H (1991) $^{40}Ar/^{39}Ar$ age and duration of tholeiitic magmatism related to the early opening of the Red Sea rift. Geophys Res Lett 18:195–198

Garfunkel Z (1988) Relation between continental rifting and uplifting: evidence from the Suez rift and northern Red Sea. Tectonophysics 150:33–49

Garfunkel Z, Bartov Y (1977) The tectonics of the Suez rift. Geol Surv Isr Bull 71:44–50

Garfunkel Z, Beyth M (2006) Constraints on the structural development of Afar imposed by the kinematics of the major surrounding plates. In: Yirgu G, Ebinger C, Maguire PKH (eds) The structure and evolution of the East African Rift System in the Afar volcanic province, vol 259. Geological Society Special Publication, London, pp 23–42

Gass IG (1970) The evolution of volcanism in the junction area of the Red Sea, Gulf of Aden and Ethiopian rifts. Philos Trans Royal Soc London A 267:369–382

Gaulier JM, Le Pichon X, Lyberis N, Avedik F, Geli L, Moretti I, Deschamps A, Salah H (1988) Seismic study of the crust of the northern Red Sea and Gulf of Suez. Tectonophysics 153:55–88

Gee JS, Kent DV (2007) Source of oceanic magnetic anomalies and the geomagnetic polarity timescale. Treatise Geophys 5:455–507

Genik GJ (1992) Regional framework, structural and petroleum aspects of rift basins in Niger, Chad and the Central African Republic (C.A.R.). Tectonophysics 213:169–185

Geoffroy L, Huchon P, Khanbari K (1998) Did Yemeni tertiary granites intrude neck zones of a stretched continental upper crust? Terra Nova 10:196–200

George R, Rogers N, Kelley S (1998) Earliest magmatism in Ethiopia: evidence for two mantle plumes in one flood basalt province. Geology 26:923–926

Gettings ME, Blank HR, Mooney WD, Healy JH (1986) Crustal structure of southwestern Saudi Arabia. J Geophys Res 91:6491–6512

Geukens F (1966) Geology of the Arabian Peninsula, Yemen. U.S. Geological Survey Professional Paper 560-B

Ghebreab W, Carter A, Hurford AJ, Talbot CJ (2002) Constraints for timing of extensional tectonics in the western margin of the Red Sea in Eritrea. Earth Planet Sci Lett 200:107–119

Gibbs AD (1984) Structural evolution of extensional basin margins. J Geol Soc London 142:609–620

Girdler RW (1958) The relationship of the Red Sea to the East African Rift system. Quar J Geol Soc London 114:79–105

Girdler RW (1966) The role of translational and rotational movements in the formation of the Red Sea and Gulf of Aden. In: The world rift system. Geological Survey of Canada, Canada paper 66-14, pp 65–77

Girdler RW (1970) A review of Red Sea heat flow. Philos Trans Roy Soc London Series A Math Phys Sci 267:191–203

Girdler RW (1991) The Afro-Arabian rift system; an overview. Tectonophysics 197:139–153

Girdler RW, Darracott BW (1972) African poles of rotation. Comments Earth Sci Geophys 2:131–138

Girdler RW, Evans TR (1977) Red sea heat flow. Geophys J Roy Astron Soc 51:245–251

Girdler RW, Southren TC (1987) Structure and evolution of the northern Red Sea. Nature 330:716–721

Girdler RW, Styles P (1974) Two-stage Red Sea floor spreading. Nature 247:7–11

Girdler RW, Underwood M (1985) The evolution of early oceanic lithosphere in the southern Red Sea. Tectonophysics 116:95–108

Girdler RW, Whitmarsh RB (1974) Miocene evaporites in Red Sea cores, their relevance to the problem of the width and age of oceanic crust beneath the Red Sea. In: Whitmarsh RB, Weser OE, Ross DA et al (eds) Initial reports of the deep sea drilling project, vol 23. Government Printing Office, Washington, pp 913–921

GLOBE Task Team and others (Hastings, David A., Paula K. Dunbar, Gerald M. Elphingstone, Mark Bootz, Hiroshi Murakami, Hiroshi Maruyama, Hiroshi Masaharu, Peter Holland, John Payne, Nevin A. Bryant, Thomas L. Logan, J.-P. Muller, Gunter Schreier, and John S. MacDonald) (eds) (1999) The global land one-kilometer base elevation (GLOBE) digital elevation model, Version 1.0. National Oceanic and Atmospheric Administration, National Geophysical Data Center, 325 Broadway, Boulder, Colorado 80303, USA

Gradstein FM, Ogg JG, Smith AG, Bleeker W, Lourens LJ (2004) A new geologic time scale, with special reference to Precambrian and Neogene. Episodes 27:83–100

Granath JW (2001) The Nogal rift of Northern Somalia: Gulf of Aden. Reactivation of a Mesozoic rift. In: Ziegler PA, Cavazza W, Robertson AHF, Crasquin-Soleau S (eds) Peri-Tethys Memoir 6: Peri-Tethyan Rift/Wrench Basins and Passive Margins vol 186, Mémoires du Muséum national d'Histoire naturelle de Paris, pp 511–527

Greenwood JEGW, Bleackley D (1967) Geology of the Arabian Peninsula, Aden Protectorate. U.S. Geological Survey Professional Paper 560-C, pp 1–96

Groenewald PB, Grantham GH, Watkeys MK (1991) Geological evidence for a Proterozoic to Mesozoic link between southeastern Africa and Dronning Maud Land, Antarctica. J Geol Soc London 148:1115–1123

Grolier MJ, Overstreet WC (1978) Geologic Map of Yemen Arab Republic (San'a). U.S. Geological Survey, Miscellaneous Inf. Series, Map 1-1143-B, scale 1:500,000

Guennoc P, Pautot G, Coutelle A (1988) Surficial structures of the northern Red Sea axial valley from 23°N to 28°N: time and space evolution of neo-oceanic structures. Tectonophysics 153:1–23

Guiraud M (1993) Late Jurassic rifting—early cretaceous rifting and late cretaceous transpressional inversion in the upper Benue basin (NE Nigeria. Bull Centres Rech Expor Prod Elf Aquitaine 17:371–383

Guiraud R, Bosworth W (1999) Phanerozoic geodynamic evolution of northeastern Africa and the northwestern Arabian platform. Tectonophysics 315:73–108

Guiraud R, Maurin J-C (1992) Early Cretaceous rifts of western and Central Africa: an overview. Tectonophysics 213:153–168

Guiraud R, Bosworth W, Thierry J, Delplanque A (2005) Phanerozoic geological evolution of Northern and Central Africa: an overview. In: Catuneanu O, Guiraud R, Eriksson P, Thomas B, Shone R, Key R (eds) Phanerozoic evolution of Africa. J Afr Earth Sci 43: 83–143

Hadley DG, Schmidt DL (1980) Sedimentary rocks and basins of the Arabian shield and their evolution. Inst Appl Geol Bull King Abdulaziz University 4:26–50

Hadley DG, Schmidt DL, Coleman (1982) Summary of tertiary investigations in western Saudi Arabia, current work by the U.S. Geological Survey, and recommended future studies. U.S. Geological Survey Open File Report USGS-OF-03-5

Hall SA, Andreason GE, Girdler RW (1977) Total intensity magnetic anomaly map of the Red Sea and adjacent coastal areas, a description and preliminary interpretation, vol 22. Saudi Arabia Directorate General Mineral Resources Bulletin, Red Sea Research 1970–1975: F1–F15

Haq BU, Hardenbol J, Vail PR (1987) Chronology of fluctuating sea-levels since the Triassic. Science 235:1156–1167

Hassan F, El-Dashlouty S (1970) Miocene evaporites of Gulf of Suez region and their significance. Am Assoc Pet Geol Bull 54:1686–1696

Heaton RC, Jackson MPA, Bamahmoud M, Nani ASO (1995) Superposed Neogene extension, contraction and salt canopy emplacement in the Yemeni Red Sea. In: Jackson MPA, Roberts DG, Snelson S (eds) Salt Tectonics: a global perspective, vol 65. American Association of Petroleum Geologists Memoir, pp 333–351

Hébert H, Deplus C, Huchon P, Khanbari K, Audin L (2001) Lithospheric structure of a nascent spreading ridge inferred from gravity data: the western Gulf of Aden. J Geophys Res 106:26345–26363

Hempton MR (1987) Constraints on Arabian plate motion and extensional history of the Red Sea. Tectonics 6:687–705

Henning AT, Sawyer DS, Templeton DS (2004) Exhumed upper mantle within the ocean-continent transition of the northern West Iberia margin: evidence from prestack depth migration and total tectonic subsidence analyses. J Geophys Res 109:B05103

Hewaidy AA, Farouk S, Ayyad HM (2012) Nukhul formation in Wadi Baba, southwest Sinai Peninsula, Egypt. GeoArabia 17:103–120

Hey R (1977) A new class of "pseudofaults" and their bearing on plate tectonics; a propagating rift model. Earth Planet Sci Lett 37:321–325

Holmes A (1965) Principles of physical geology, 2nd edn. Thomas Nelson Ltd, Edinburgh, 1288 pp

Hutchinson RW, Engels GG (1970) Tectonic significance of regional geology and evaporite lithofacies in northeastern Ethiopia. Philos Trans Roy Soc London Series A Math Phys Sci 267:313–329
Hutchinson RW, Engels GG (1972) Tectonic evolution in the southern Red Sea and its possible significance to older rifted continental margins. Geol Soc Am Bull 83:2989–3002
Hughes GW, Beydoun ZR (1992) The Red Sea-Gulf of Aden: biostratigraphy, lithostratigraphy and palaeoenvironments. J Pet Geol 15:135–156
Hughes GW, Filatoff J (1995) New biostratigraphic constraints on Saudi Arabian Red Sea pre- and syn-rift sequences. In: Al-Husseini MI (ed) Middle east petroleum geosciences, Geo'94, vol 2. Gulf PetroLink, Bahrain, pp 517–528
Hughes GW, Johnson RS (2005) Lithostratigraphy of the Red Sea region. GeoArabia 10:49–126
Hughes GW, Abdine S, Girgis MH (1992) Miocene biofacies development and geological history of the Gulf of Suez, Egypt. Mar Pet Geol 9:2–28
Hughes GW, Perincek D, Grainger DJ, Abu-Bshait A-J, Jarad A-RM (1999) Lithostratigraphy and depositional history of part of the Midyan region, northwestern Saudi Arabia. GeoArabia 4:503–541
Hughes GW, Varol O, Beydoun ZR (1991) Evidence for Middle Oligocene rifting of the Gulf of Aden and for Late Oligocene rifting of the southern Red Sea. Mar Pet Geol 8:354–358
Hume WF, Madgwick TG, Moon FW, Sadek H (1920) Preliminary geological report on the Gebel Tanka area, vol 4. Petroleum Research Bulletin, 16 pp
Ilani S, Harlavan Y, Tarawneh K, Rabba I, Weinberger R, Ibrahim K, Peltz S, Steinitz G (2001) New K-Ar ages of basalts from the Harrat Ash Shaam volcanic field in Jordan: implications for the span and duration of the upper-mantle upwelling beneath the western Arabian plate. Geology 29:171–174
Issawi B, El Hinnawi M, Francis M, Mazhar A (1999) The Phanerozoic geology of Egypt: a geodynamic approach. Egypt Geological Survey Paper 76, 462 pp
Jackson CAL (2008) Sedimentology and significance of an early syn-rift paleovalley, Wadi Tayiba, Suez Rift, Egypt. J Afr Earth Sci 52:62–68
Jackson CAL, Gawthorpe RL, Leppard CW, Sharp IR (2006) Rift-initiation development of normal fault blocks: insights from the Hammam Faraun fault block, Suez rift, Egypt. J Geol Soc London 163:165–183
Janssen ME, Stephenson RA, Cloetingh S (1995) Temporal and spatial correlations between changes in plate motions and the evolution of rifted basins in Africa. Geol Soc Am Bull 107:1317–1332
Jarrige JJ, Ott d'Estevou P, Burollet PF, Montenat C, Prat P, Richert JP, Thiriet JP (1990) The multistage tectonic evolution of the Gulf of Suez and northern Red Sea continental rift from field observations. Tectonics 9:441–465
Jarrige JJ, Ott d'Estevou P, Burollet PF, Thiriet JP, Icart JC, Richert JP, Sehans P, Montenat C, Prat P (1986) Inherited discontinuities and Neogene structure: the Gulf of Suez and northwestern edge of the Red Sea. Philos Trans R Soc Lond A317:129–139
Joffe S, Garfunkel Z (1987) Plate kinematics of the circum Red Sea—a re-evaluation. Tectonophysics 141:5–22
Jolivet L, Faccenna C (2000) Mediterranean extension and the Africa–Eurasia collision. Tectonics 19:1095–1106
Juteau T, Eissen J, Monin AS, Zonenshain (Zonenshayn) LP, Sorokhtin OG, Matveenkov (Matveyenko) VV, Almukhamedov A (1983) Structure et petrologie du rift axial de la Mer Rouge vers 18 degrees Nord: Resultats de la campagne sovietique de plongees avec submersible (1980). Bulletin Des Centres De Recherches Exploration-Production Elf-Aquitaine 7, pp 217–231
Kappelman J, Simons L, Swisher CC III (1992) New age determinations for the Eocene-Oligocene boundary sediments in the Fayum depression, northern Egypt. J Geol 100:647–668
Karner G, Driscoll NW, Barker DHN (2003) Syn-rift regional subsidence across the West African continental margin: the role of lower plate ductile extension. In: Arthur TJ, MacGregor DS, Cameron NR (eds) Petroleum geology of Africa: new themes and developing technologies, vol 207. Geological Society Special Publications, London, pp 105–129
Kassas M, Zahran MA (1971) Plant life on the coastal mountains of the Red Sea, Egypt. J Indian Bot Soc Golden Jubilee 50A:571–589
Kazmin VG (1973) Geological map of Ethiopia, scale 1:2,000,000. Ministry of Mines, Geological Survey of Ethiopia, Addis Ababa
Kazmin VG (1977) Characteristics of geodynamic evolution of the Afro-Arabian rift system. Izd. Nauka, Sib. Otd, Novosibirsk (in Russian)
Kenea NH, Ebinger CJ, Rex DC (2001) Late Oligocene volcanism and extension in the southern Red Sea Hills, Sudan. J Geol Soc London 158:285–294
Khalil SM (1998) Tectonic evolution of the eastern margin of the Gulf of Suez, Egypt. PhD thesis, Royal Holloway, University of London, 349 pp
Khalil SM, McClay KR (2009) Structural control on syn-rift sedimentation, northwestern Red Sea margin, Egypt. Mar Pet Geol 26:1018–1034
Khan MA (1975) The Afro-Arabian rift system. Science Progress (1916) 62: 207–236
Khedr E (1984) Sedimentological evolution of the Red Sea continental margin of Egypt and its relationship to sea-level changes. Sed Geol 39:71–86
Klitgord KD, Schouten H (1986) Plate kinematics of the Central Atlantic. In: Vogt PR, Tucholke BE (eds) The Western North Atlantic Region (The Geology of North America, v. M). Geological Society of America, pp 351–378
Klitzsch E (1990) Chapter 21. Paleozoic. In: Said R (ed) The geology of Egypt. Balkema, Rotterdam, pp 393–406
Klitzsch E, List FK, Pohlmann G, Handley R, Hermina M, Meissner G (eds) (1986, 1987) Geological map of Egypt: 1:50,000 scale, 20 sheets. Conoco and Egyptian General Petroleum Corporation, Cairo
Kohn BP, Eyal M (1981) History of uplift of the crystalline basement of Sinai and its relation to opening of the Red Sea as revealed by fission track dating of apatites. Earth Planet Sci Lett 52:129–141
Krenkel E (1922) Die Bruchzonen Ostafrikas: Tektonik, Vulkanismus, Erdbeben und Schwereanomalien. Verlag von Gebrüder Borntraeger, Berlin, 184 pp
Krenkel E (1957) Geologie und Bodenschätze Afrikas, 2nd edn. Geest and Portig, Leipzig, 597 pp
Larsen P (1988) Relay structures in a Lower Permian basement-involved extension system, East Greenland. J Struct Geol 10:3–8
Lambiase JJ, Bosworth W (1995) Structural controls on sedimentation in continental rifts. In: Lambiase JJ (ed) Hydrocarbon habitat in rift basins, vol 80. Geological Society Special Publication, London, pp 117–144
Laughton AS (1970) A new bathymetric chart of the Red Sea. Philos Trans Roy Soc London Series A Math Phys Sci 267:21–22
Lazar M, Ben-Avraham Z, Garfunkel Z (2012) The Red Sea—new insights from recent geophysical studies and the connection to the Dead Sea fault. J Afr Earth Sc 68:96–110
Le Pichon X, Francheteau J (1978) A plate tectonic analysis of the Red Sea—Gulf of Aden area. Tectonophysics 46:369–406
Le Pichon X, Sibuet J (1981) Passive margins: a model of formation. J Geophys Res 86:3708–3720
Leroy S, Gente P, Fournier M, d'Acremont E, Patriat P, Beslier M-O, Bellahsen N, Maia M, Blais A, Perrot J, Al-Kathiri A, Merkouriev S, Fleury J-M, Ruellan P-Y, Lepvrier C, Huchon P (2004) From rifting to spreading in the eastern Gulf of Aden: a geophysical survey of a young oceanic basin from margin to margin. Terra Nova 16:185–192
Lithgow-Bertelloni C, Richards MA (1998) The dynamics of Cenozoic and Mesozoic plate motions. Rev Geophys 36:27–78

Lotfy HI, Van der Voo R, Hall CM, Kamel OA, Abdel Aal AY (1995) Palaeomagnetism of Early Miocene basaltic eruptions in the areas east and west of Cairo. J Afr Earth Sci 21:407–419

Lowell JD, Genik GJ (1972) Sea-floor spreading and structural evolution of southern Red Sea. Am Assoc Pet Geol Bull 56:247–259

Lyakhovsky V, Segev A, Schattner U, Weinberger R (2012) Deformation and seismicity associated with continental rift zones propagating toward continental margins. Geochem Geophys Geosyst 13:Q01012

Makris J, Allam A, Moller L (1981) Deep seismic studies in Egypt and their interpretation. EOS Trans Am Geophys Union 62:230

Makris J, Henke CH, Egloff F, Akamaluk T (1991a) The gravity field of the Red Sea and East Africa. Tectonophysics 198:269–381

Makris J, Tsironidis J, Richter H (1991b) Heatflow density distribution in the Red Sea. Tectonophysics 198:383–393

Manighetti I, Tapponnier P, Courtillot V, Gruszow S, Gillot PY (1997) Propagation of rifting along the Arabia-Somalia plate boundary: the Gulfs of Aden and Tadjoura. J Geophys Res 102:2681–2710

Martin AK (1984) Propagating rifts: crustal extension during continental rifting. Tectonics 3:611–617

Martinez F, Cochran JR (1988) Structure and tectonics of the northern Red Sea: catching a continental margin between rifting and drifting. Tectonophysics 150:1–32

Martinez F, Cochran JR (1989) Geothermal measurements in the northern Red Sea: implications for lithospheric thermal structure and mode of extension during continental rifting. J Geophys Res 94:12239–12266

Martini E (1971) Standard tertiary and quaternary calcareous nannoplankton zonation. In: Farinacci A (ed) Proceedings of the 2nd planktonic conference, Roma, 1970, Tecnoscienza, Roma, pp 739–785

Mattash MA (2008) Younger volcanic fields of Yemen with focus on Jabal at-Tair active volcano in the Red Sea. In: International Geological Congress Abstracts, vol 33, Abstract 1287199

Mathews DH, Williams CA, Laughton AS (1967) Mid-ocean ridge in the mouth of the Gulf of Aden. Nature 215:1052–1053

McClay KR, Nicols GJ, Khalil SM, Darwish M, Bosworth W (1998) Extensional tectonics and sedimentation, eastern Gulf of Suez, Egypt. In: Purser BH, Bosence DWJ (eds) Sedimentation and tectonics of rift basins: Red Sea-Gulf of Aden. Chapman and Hall, London, pp 223–238

McGuire AV, Bohannon RG (1989) Timing of mantle upwelling; evidence for a passive origin for the Red Sea Rift. J Geophys Res 94:1677–1682

McGuire AV, Coleman RG (1986) The Jabal Tirf layered gabbro and associated rocks of the Tihama Asir Complex, SW Saudi Arabia. J Geol 94:651–665

McKenzie DP, Davies D, Molnar P (1970) Plate tectonics of the Red Sea and East Africa. Nature 226:243–248

McQuarrie N, Stock JM, Verdel C, Wernicke BP (2003) Cenozoic evolution of Neotethys and implications for the causes of plate motions. Geophys Res Lett 30:2036

Federal MDA (2004) Landsat GeoCover ETM + 2000 Edition Mosaics. USGS, Sioux Falls, South Dakota 2000

Menzies MA, Baker J, Bosence D, Dart C, Davidson I, Hurford A, Al Kadasi M, McClay K, Nichols G, Al Subbary A, Yelland A (1992) The timing of magmatism, uplift and crustal extension: preliminary observations from Yemen. In: Storey BC, Alabaster T, Pankhurst RJ (eds) Magmatism and the causes of continental break-up, vol 68. Geological Society Special Publication, London, pp 293–304

Menzies M, Gallagher K, Yelland A, Hurford AJ (1997) Volcanic and non-volcanic rifted margins of the Red Sea and Gulf of Aden: crustal cooling and margin evolution in Yemen. Geochimica Cosmochimica Acta 61:2511–2527

Milanovsky EE (1972) Continental rift zones: their arrangement and development. Tectonophysics 15:65–70

Milkereit B, Fluh ER (1985) Saudi Arabian refraction profile; crustal structure of the Red Sea-Arabian shield transition. Tectonophysics 111:283–298

Miller PM, Barakat H (1988) Geology of the Safaga concession, northern Red Sea, Egypt. Tectonophysics 153:123–136

Mohn G, Manatschal G, Beltrando M, Masini E, Kusznir N (2012) Necking of continental crust in magma-poor rifted margins: evidence from the fossil Alpine Tethys margins. Tectonics 31:TC1012

Mohr PA (1970) The Afar triple junction and sea-floor spreading. J Geophys Res 75:7340–7352

Monin AS, Litvin VM, Podreazhansky AM, Sagalevich AM, Sorokhtin OG, Voitov VI, Yastrebov VS, Zonenshain LP (1982) Red Sea submersible research expedition. Deep Sea Res 29:361–373

Monin AS, Plakhin EA, Podrazhansky AM, Sagalevich AM, Sorokhtin OG (1981) Visual observations of the Red Sea hot brines. Nature 291:222–225

Mooney WD, Gettings ME, Blank HR, Healy JH (1985) Saudi Arabian seismic-refraction profile; a traveltime interpretation of crustal and upper mantle structure. Tectonophysics 111:173–246

Moretti I, Chénet PY (1987) The evolution of the Suez rift: a combination of stretching and secondary convection. Tectonophysics 133:229–234

Moretti I, Colletta B (1988) Fault block tilting: the Gebel Zeit example, Gulf of Suez. J Struct Geol 10:9–19

Morgan P, Swanberg CA, Boulos FK, Hennin SF, El Sayed AA, Basta NZ (1980) Geothermal studies in Northeast Africa. Ann Geol Surv Egypt 10:971–987

Morley CK, Nelson RA, Patton TL, Munn SG (1990) Transfer zones in the east African rift system and their relevance to hydrocarbon exploration in rifts. Am Assoc Pet Geol Bull 74:1234–1253

Mougenot D, Al-Shakhis AA (1999) Depth imaging sub-salt structures: a case study in the Midyan Peninsula (Red Sea). GeoArabia 4:335–463

Moustafa AM (1976) Block faulting of the Gulf of Suez. In: 5th Egyptian General Petroleum Organization Exploration Seminar, Cairo, 19 pp (unpublished report distributed as paper copies at the conference)

Moustafa AR (1997) Controls on the development and evolution of transfer zones: the influence of basement structure and sedimentary thickness in the Suez rift and Red Sea. J Struct Geol 19:755–768

Mulder CJ, Lehner P, Allen DCK (1975) Structural evolution of the Neogene salt basins in the eastern Mediterranean and the Red Sea. Geol Mijnbouw 54:208–221

Musser JA, Al-Amri M, Al-Omar W, Lafon SK, Arifin M (2012) Wide azimuth towed streamer 3-D seismic in the Red Sea. Middle East geosciences conference and exhibition 10, 4–7 March, Bahrain, abstracts

Omar GI, Steckler MS (1995) Fission track evidence on the initial rifting of the Red Sea: two pulses, no propagation. Science 270:1341–1344

Omar GI, Steckler MS, Buck WR, Kohn BP (1989) Fission-track analysis of basement apatites at the western margin of the Gulf of Suez rift, Egypt: evidence for synchronicity of uplift and subsidence. Earth Planet Sci Lett 94:316–328

Orszag-Sperber F, Harwood G, Kendall A, Purser BH (1998) A review of the evaporites of the Red Sea-Gulf of Suez rift. In: Purser BH, Bosence DWJ (eds) Sedimentation and tectonics of rift basins: Red Sea-Gulf of Aden. Chapman and Hall, London, pp 409–426

Patton TL, Moustafa AR, Nelson RA, Abdine SA (1994) Tectonic evolution and structural setting of the Suez Rift. In: Landon SM (ed) Interior rift basins. American Association of Petroleum Geologists Memoir 59, pp 7–55

Pautot G (1983) Les fosses de la Mer Rouge: Approche geomorphologique d'un stade initial d'ouvertur oceanique realisee a l'aide du Seabeam. Oceanol Acta 6:235–244

Pautot G, Guennoc P, Coutelle A, Lyberis N (1984) Discovery of a large brine deep in the northern Red Sea. Nature 310:133–136

Peacock DCP, Sanderson DJ (1991) Displacements, segment linkage and relay ramps in normal fault zones. J Struct Geol 13:721–733

Perry SK, Schamel S (1990) The role of low-angle normal faulting and isostatic response in the evolution of the Suez rift, Egypt. Tectonophysics 174:159–173

Phillips JD (1970) Magnetic anomalies in the Red Sea. Philos Trans Roy Soc London Series A Math Phys Sci 267:205–217

Plaziat JC, Montenat C, Barrier P, Janin MC, Orszag-Sperber F, Philobbos E (1998) Stratigraphy of the Egyptian syn-rift deposits: correlations between axial and peripheral sequences of the north-western Red Sea and Gulf of Suez and their relations with tectonics and eustacy. In: Purser BH, Bosence DWJ (eds) Sedimentation and Tectonics in Rift Basins—Red Sea—Gulf of Aden. Chapman and Hall, London, pp 211–222

Prodehl C (1985) Interpretation of a seismic-refraction survey across the Arabian Shield in western Saudi Arabia. Tectonophysics 111:247–282

Quennell AM (1951) Geology and mineral resource of (former) Transjordan. Colonial Geol Miner Res 2:85–115

Quennell AM (1958) The structural and geomorphic evolution of the Dead Sea Rift. Quar J Geol Soc London 114:1–24

Rabinowitz PD, Coffin MF, Falvey D (1983) The separation of Madagascar and Africa. Science 220:67–69

Rabinowitz PD, LaBreque J (1979) The Mesozoic South Atlantic Ocean and evolution of its continental margins. J Geophys Res 84:5973–6003

Redfield TF, Wheeler WH, Often M (2003) A kinematic model for the development of the Afar depression and its paleogeographic implications. Earth Planet Sci Lett 216:383–398

Reeves CV, Karanja FM, Macleod IN (1987) Geophysical evidence for a failed Jurassic Rift and triple junction in Kenya. Earth Planet Sci Lett 81:231–299

Reilinger R, McClusky S (2011) Nubia-Arabia-Eurasia plate motions and the dynamics of Mediterranean and Middle East tectonics. Geophys J Int 186:971–979

Richardson M, Arthur MA (1988) The Gulf of Suez–northern Red Sea Neogene rift: a quantitive basin analysis. Mar Pet Geol 5:247–270

Robertson AHF, Bamakhalif KAS (1998) Late Oligocene–early Miocene rifting of the northeastern Gulf of Aden: basin evolution in Dhofar (southern Oman). In: Ziegler PA, Cavazza W, Robertson AHF, Crasquin-Soleau S (eds) Peri-Tethys Memoir 6: Peri-Tethyan Rift/Wrench Basins and Passive Margins, Mémoires du Muséum National d'Histoire Naturelle de Paris 186, pp 641–670

Robertson AHF, Dixon JE, Brown S, Collins A, Morris A, Pickett E, Sharp I, Ustaömer T (1996) Alternative tectonic models for the Late Palaeozoic–Early Tertiary development of Tethys in the Eastern Mediterranean region. In: Morris A, Tarling DH (eds) Palaeomagnetism and Tectonics of the Mediterranean Region. Geological Society Special Publication, London, 105, pp 239–263

Rochette P, Tamrat E, Féraud G, Pik R, Courtillot V, Kefeto E, Coulon C, Hoffmann C, Vandamme D, Yirgu E (1997) Magnetostratigraphy and timing of the Oligocene Ethiopian traps. Earth Planet Sci Lett 164:497–510

Roger J, Platel JP, Cavelier C, Bourdillon-de-Grisac C (1989) Données nouvelles sur la stratigraphie et l'histoire géologique du Dhofar (Sultanat d'Oman). Bulletin de la Société géologique de France 8:265–277

Rosendahl BR, Reynolds DJ, Lorber PM, Burgess CF, McGill J, Scott D, Lambiase JJ, Derksen SJ (1986) Structural expressions of rifting: Lessons from Lake Tanganyika, Africa. In: Frostick LE, Renaut RW, Reid I, Tiercelin JJ (eds) Sedimentation in the African Rifts, vol 25. Geological Society Special Publications London, pp 29–43

Röser HA (1975) A detailed magnetic survey of the southern Red Sea. Geologie Jahrbuch 13:131–153

Ross DA, Schlee J (1973) Shallow structure and geologic development of the southern Red Sea. Geol Soc Am Bull 84:3827–3848

Ross DA, Whitmarsh RB, Ali SA, Boudreaux JE, Coleman RG, Fleisher RL, Girdler RW, Manheim F, Matter A, Ngrini C, Stoffers P, Supko PR (1973) Red Sea drillings. Science 179:377–380

Sagri M, Abbate E, Azzaroli A, Balestrieri ML, Benvenuti M, Bruni P, Fazzuoli M, Ficcarelli G, Marcucci M, Papini M, Pavia G, Reale V, Rook L, Tecle TM (1998) New data on the Jurassic and Neogene sedimentation in the Danakil Horst and northern Afar Depression, Eritrea. In: Crasquin-Soleau S, Barrier É (eds) Peri-Tethys Memoir 3: stratigraphy and evolution of Peri-Tethyan platforms, vol 177. Mémoires du Muséum National d'Histoire Naturelle de Paris, pp 193–214

Sahota G (1990) Geophysical investigations of the Gulf of Aden continental margins: geodynamic implications for the development of the Afro-Arabian Rift system. PhD thesis, University College, Swansea, UK

Saleh S, Jahr T, Jentzsch G, Saleh A, Abou Ashour NM (2006) Crustal evaluation of the northern Red Sea rift and Gulf of Suez, Egypt from geophysical data: 3-dimensional modeling. J Afr Earth Sci 45:257–278

Saoudi A, Khalil B (1986) Distribution and hydrocarbon potential of Nukhul sediments in the Gulf of Suez. In: Proceedings of the 7th exploration seminar, vol 1, Egyptian General Petroleum Corporation, Cairo, March 1984, pp 75–96

Savoyat E, Shiferaw A, Balcha T (1989) Petroleum exploration in the Ethiopian Red Sea. J Pet Geol 12:187–204

Schandelmeier H, Reynolds PO, (1997) Palaeogeographic–Palaeotectonic Atlas of North-Eastern Africa, Arabia and Adjacent Areas. Balkema, Rotterdam, 160 pp, 17 plates

Scheuch J (1976) Preliminary heat flow map of the Red Sea and an attempt to provide a geological-geophysical interpretation. In: Pilger A, Roesler A (eds) Afar between Continental and Oceanic Rifting, vol 2, E. Schweizerbart Verlagsbuchhandl (Naegele u. Obermiller), Stuttgart: pp 171−174

Schmidt DL, Hadley DG, Brown GF (1983) Middle Tertiary continental rift and evolution of the Red Sea in southwestern Saudi Arabia. U.S. Geological Survey Open File Report 83-0641

Searle RC, Ross DA (1975) A geophysical study of the Red Sea axial trough between 20.5° and 22°N. Geophys J Roy Astron Soc 43:555–572

Sebai A, Zumbo V, Féraud G, Bertrand H, Hussain AG, Giannerini G, Campredon R (1991) 40Ar/39Ar dating of alkaline and tholeiitic magmatism of Saudi Arabia related to the early Red Sea rifting. Earth Planet Sci Lett 104:473–487

Segev A, Rybakov M (2011) History of faulting and magmatism in the Galilee (Israel) and across the Levant continental margin inferred from potential field data. J Geodyn 51:264–284

Sellwood BW, Netherwood RE (1984) Facies evolution in the Gulf of Suez area: sedimentation history as an indicator of rift initiation and development. Modern Geol 9:43–69

Şengör AMC (2001) Elevation as indicator of mantle-plume activity. In: Ernst RE, Buchan KL (eds) Mantle plumes: their identification through time. Geological Society of America Special Paper 352, pp 183–225

Şengör AMC, Burke K (1978) Relative timing of rifting on earth and its tectonic implications. Geophys Res Lett 5:419–421

Şengör AMC, Yilmaz Y (1981) Tethyan evolution of Turkey: a plate tectonic approach. Tectonophysics 75:181–241

Shackleton NJ, Berger A, Peltier WR (1990) An alternative astronomical calibration of the lower Pleistocene timescale based on ODP Site 677. Trans Roy Soc Edinburgh Earth Sci 81:251–261

Sharp IR, Gawthorpe RL, Underhill JR, Gupta S (2000) Fault propagation folding in extensional settings: examples of structural

style and synrift sedimentary response from the Suez rift, Sinai, Egypt. Geol Soc Am Bull 112:1877–1899
Smith WHF, Sandwell DT (1997) Global sea floor topography from satellite altimetry and ship depth soundings. Sci Mag 277:1956–1962
Spohner R, Oleman P (1986) Topography, Red Sea Region (1:8,000,000). German Research Foundation, Karlsruhe
Stampfli GM, Borel GD (2002) A plate tectonic model for the Paleozoic and Mesozoic constrained by dynamic plate boundaries and restored synthetic oceanic isochrons. Earth Planet Sci Lett 196:17–33
Stampfli GM, Mosar J, Favre P, Pillevuit A, Vannay J-C (2001) Permo-Mesozoic evolution of the western Tethys realm: the Neo- Tethys East Mediterranean Basin connection. In: Ziegler PA, Cavazza W, Robertson AHF, Crasquin-Soleau S (eds) Peri-Tethys Memoir 6: Peri-Tethyan Rift/Wrench Basins and Passive Margins, vol 186, Mémoires du Muséum national d'Histoire naturelle de Paris, pp 51–108
Steckler MS (1985) Uplift and extension at the Gulf of Suez: indications of induced mantle convection. Nature 317:135–139
Steckler MS, Omar I (1994) Controls on erosional retreat of the uplifted rift flanks at the Gulf of Suez and northern Red Sea. J Geophys Res 99:1–2
Steckler MS, ten Brink US (1986) Lithospheric strength variations as a control on new plate boundaries: examples from the northern Red Sea region. Earth Planet Sci Lett 79:120–132
Steckler MS, Berthelot F, Lyberis N, Le Pichon X (1988) Subsidence in the Gulf of Suez: implications for rifting and plate kinematics. Tectonophysics 153:249–270
Steckler M, Cochran J, Bosworth W (2001) Rupturing of continental lithosphere in the northern and central Red Sea/Gulf of Suez region: workshop report. Margins Newsl 6:5–9
Stein CA, Cochran JR (1985) The transition between the Sheba Ridge and Owen Basin: rifting of old oceanic Lithosphere. Geophys J Roy Astron Soc 81:47–74
Sutra E, Manatschal G (2012) How does the continental crust thin in a hyperextended rifted margin? insights from the Iberia margin. Geology 40:139–142
Szymanski E (2013) Timing, kinematics and spatial distribution of Miocene extension in the central Arabian margin of the Red Sea rift system. PhD thesis, University of Kansas, Lawrence, 430 pp
Tefera M, Chernet T, Haro W (1996) Explanation of the geological map of Ethiopia. Ethiopian Institute of Geological Surveys, Addis Ababa 3, 79 pp
Tewfik N, Ayyad M (1984) Petroleum exploration in the Red Sea shelf of Egypt. Proc. 6th Exploration Seminar, Egyptian General Petroleum Corporation and Egypt Petroleum Exploration Society, Cairo, March 1982, 1, pp 159–180
Uchupi E (1989) The tectonic style of the Atlantic Mesozoic rift system. J Afr Earth Sci 8:143–164
Ukstins IA, Renne PR, Wolfenden E, Baker J, Ayalew D, Menzies M (2002) Matching conjugate volcanic rifted margins: $^{40}Ar/^{39}Ar$ chrono-stratigraphy of pre- and syn-rift bimodal flood volcanism in Ethiopia and Yemen. Earth Planet Sci Lett 198:289–306
U.S. Geological Survey-Arabian American Oil Company (1963) Geologic map of the Arabian Peninsula. U.S.G.S. Miscellaneous Geological Investigations Map I-270-A, 1:2,000,000 scale. U.S. Geological Survey, Washington
Vail JR (1975) Geologic map; the Democratic Republic of Sudan and adjacent areas, scale 1:2,000,000. Survey Review, Tolworth
Vail JR (1978) Outline of the geology and mineral deposits of the Democratic Republic of the Sudan and adjacent areas. Overseas geology and mineral resources 49 (includes the Geologic Map of Sudan, scale 1:2:000,000, north and south sheets 1203A and 1203B), 68 pp
Van Wijk JW, Blackman DK (2005) Dynamics of continental rift propagation: the end-member modes. Earth Planet Sci Lett 229:247–258
Varet J (1978) In: Gasse F (ed) Geology of central and southern Afar (Ethiopia and Djibouti Republic). CNRS, Paris, 118 pp
Vellutini P (1990) The Manda-Inakir Rift, Republic of Djibouti: a comparison with the Asal Rift and its geodynamic interpretation. Tectonophysics 172:141–153
Vening Meinesz FA (1934) Gravity Expeditions at Sea. vol 2 (1923–1932). Publications Netherlands Geodetic Commission, Delft
Vink GE (1982) Continental rifting and the implications for plate tectonic reconstructions. J Geophys Res 87:10677–10688
Vink GE, Morgan WJ, Zhao W-L (1984) Preferential rifting of continents: a source of displaced terranes. J Geophys Res 89:10072–10076
Voggenreiter W, Hötzl H, Mechie J (1988) Low-angle detachment origin for the Red Sea Rift system? Tectonophysics 150:51–75
Von Triulzi AE (1898) Expedition S.M. Schiff Pola in das Rothe Meer, nördliche Hälfte, Wissenschaftliche Ergebnisse, XII, Relative Schwerebestimmung. Denkschriften der Kaiserlichen Akademie der Wissenschaften, Mathematisch – Naturwissenschaftliche Klasse 65, pp 131–206
Watchorn F, Nichols GJ, Bosence DWJ (1998) Rift-related sedimentation and stratigraphy, southern Yemen (Gulf of Aden). In: Purser BH, Bosence DWJ (eds) Sedimentation and tectonics of rift basins: Red Sea-Gulf of Aden. Chapman and Hall, London, pp 165–189
Wernicke B (1985) Uniform-sense normal simple shear of the continental lithosphere. Can J Earth Sci 22:108–125
Wescott WA, Krebs WN, Dolson JC, Ramzy M, Karamat SA, Moustafa T (1997) Chronostratigraphy, sedimentary facies, and architecture of tectono-stratigraphic sequences: an integrated approach to rift basin exploration, Gulf of Suez, Egypt. In: Shanley KW, Perkins BF (eds) Gulf coast section SEPM foundation 18th annual research conference, Shallow Marine and Nonmarine Reservoirs, 7–10 Dec 1997, pp 377–399
Whitmarsh RB, Manatschal G, Minshull TA (2001) Evolution of magma-poor continental margins from rifting to seafloor spreading. Nature 413:150–154
Whitmarsh RB, Weser OE, Ross DA et al. (1974) Initial reports of the Deep Sea Drilling Project, Red Sea, vol 23, U.S. Government Printing Office, Washington, 1180 pp
Williams G, Small J (1984) A study of the Oligo-Miocene basalts in the Western Desert. In: Proceedings of the 7th exploration seminar, Egyptian General Petroleum Corporation, March 1984, pp 252–268
Woodruff F, Savin SM (1989) Miocene deepwater oceanography. Paleoceanography 4:87–140
Wycisk P, Klitzsch E, Jos C, Reynolds O (1990) Intracratonal sequence development and structural control of Phanerozoic strata in Sudan. Berl Geowiss Abh A 120:45–86
Younes AI, McClay KR (2002) Development of accommodation zones in the Gulf of Suez-Red Sea rift, Egypt. Am Assoc Pet Geol Bull 86:1003–1026
Young MJ, Gawthorpe RL, Sharp IR (2000) Sedimentology and sequence stratigraphy of a transfer zone coarse-grained delta, Miocene Suez Rift, Egypt. Sedimentology 47:1081–1104
Zahran MA, Willis AJ (2009) The vegetation of Egypt, 2nd edn. Springer, Netherlands, 437 pp
Zanettin B, Justin-Visentin E, Piccirillo EM (1978) Volcanic succession, tectonics and magmatology in central Ethiopia. Atti MemAccad Patavina Sci Lett Arti 90:5–19
Ziegler MA (2001) Late Permian to Holocene paleofacies evolution of the Arabian plate and its hydrocarbon occurrences. GeoArabia 6:504–665
Zumbo V, Féraud G, Bertrand H, Chazot G (1995) $^{40}Ar/^{39}Ar$ chronology of Tertiary magmatic activity in southern Yemen during the early Red Sea-Aden rifting. J Volcanol Geoth Res 65:265–279